HYBRID LUMP-ELEMENT MICROSTRIP FILTERS

HO YI SING

A project report submitted in partial fulfilment of the requirements for the award of Bachelor of Engineering (Hons.) Electronic and Communications Engineering

Faculty of Engineering and Science
Universiti Tunku Abdul Rahman

May 2012

DECLARATION

I hereby declare that this project report is based on my original work except for citations and quotations which have been duly acknowledged. I also declare that it has not been previously and concurrently submitted for any other degree or award at UTAR or other institutions.

Signature : _________________________

Name : HO YI SING

ID No. : 08UEB06608

Date : _________________________

APPROVAL FOR SUBMISSION

I certify that this project report entitled **"HYBRID LUMP ELEMENT MICROSTRIP FILTERS"** was prepared by **HO YI SING** has met the required standard for submission in partial fulfilment of the requirements for the award of Bachelor of Electronic and Communications Engineering (Hons.) at Universiti Tunku Abdul Rahman.

Approved by,

Signature : ___________________________

Supervisor : Dr. Lim Eng Hock

Date : ___________________________

The copyright of this report belongs to the author under the terms of the copyright Act 1987 as qualified by Intellectual Property Policy of University Tunku Abdul Rahman. Due acknowledgement shall always be made of the use of any material contained in, or derived from, this report.

© 2012, Ho Yi Sing. All right reserved.

Specially dedicated to
my beloved parents and friends

ACKNOWLEDGEMENTS

I would like to thank everyone who had contributed to the successful completion of this project. I would like to express my gratitude to my research supervisor, Dr. Lim Eng Hock for his invaluable advice, guidance and his enormous patience throughout the development of the research.

In addition, I would also like to express my gratitude to my loving parent and friends who had helped and given me encouragement. Furthermore, I would like to special thanks to UTAR management. Experiments' equipment, devices and material are prepared well. Besides that, the OPAC system is very useful for me to get the journals from the Institute of Electronic and Electrical Engineering (IEEE) database. Last but not least, I would like to thank to the laboratory assistants that gave me a hand during my project.

HYBRID LUMP ELEMENT MICROSTRIP FILTERS

ABSTRACT

In this thesis lump-element method for miniaturisation of microstrip patch without degrading its radiation characteristics is investigated. It involves replacing lumped element to form microstrip coupled line filters, microstrip power dividers and microstrip rings which are investigated numerically and experimentally. Filters are usually used to let the selected frequencies to pass and reject other unwanted frequencies through the devices. Power dividers are used to couple electromagnetic signal from a transmission line to another. There are three major stages in this project: simulation, fabrication and experiment. Ansoft High Frequency Structure Simulator (HFSS) version 8 software has been used in this project in order to simulate the BPF performance for different configurations. With the help of a software, the width of the 50ohm transmission line is calculated. Advanced Wiring Revolution Design Environment (AWR) software is also used to model the proposed configurations of my project. The results are compared with those generated by the HFSS software. Experiment will be conducted to verify the simulation and measured by using the Vector Network Analyzer (VNA) in the laboratory. The computed results are compared with experimental data and again good agreement is obtained. Several case studies have been done on the proposed configuration in order to study the relationship between different values of lump-elements. The proposed project designs should be useful for reduce size in designing filter, power divider and ring.

TABLE OF CONTENTS

LIST OF TABLES

LIST OF FIGURES

LIST OF SYMBOLS / ABBREVIATIONS

λ	wavelength, m
f	frequency, Hz
c	speed of light, m/s
ε_r	dielectric constant
ε_{eff}	effective dielectric constant
h	thickness of substrate, mm
w	width of striplines, mm
Z_0	characteristic impedance, Ω
Z_{in}	input impedance, Ω
S_{11}	reflection loss, dB
S_{21}	insertion loss, dB

LIST OF APPENDICES

CHAPTER 1

INTRODUCTION

1.1 Background

The concept of microstrip antenna discussed by Deschamps in 1953 has been studied and developed extensively since 1974. They are suitable for many applications where low profile, light weight, low cost, simple geometry, compatibility with integrated circuit and conformability in the mounting of the host body are required.

There are more than 600 microstrip filter publications through IEEE Xplore in recent 10 years, and these publications continue to increase rapidly, showing a positive and strong growth in research in these areas. The rectangular patch is the most commonly used microstrip antenna, and characterised by its length and width.

In planar microstrip and stripline realization, one of the most common implementation methods for bandpass filters with required bandwidths up to a 40% of central frequency is to use a cascade of parallel-coupled sections. To utilize the spectrum resources more effectively, a bandpass filter with a wider band is more preferable. This is because more frequency components are able to get through in a single spectrum.

In addition, the filter size is also one of the concerns in the filter design. It is no doubt that smaller filters are more preferable than the bigger filters in order to easily fit into the electronic devices. Microwave filter designers have attempted to produce a wide band-pass filter through employing the multi-mode technique. The multi - mode technique has very important applications in microwave filter design for implementing miniaturization, wideband and nicer performance.

The synthesis procedure which consists of the design equation for the coupled line physical parameters (space-gap between parallel lines, line widths and lengths) is easy and can be found in any classical microwave books. The filter can be fabricated easily and it exhibits reasonably good performance compared with other planar circuit filters.

In this project, lump microstrip coupled line filter (one capacitor), lump microstrip coupled line filter (three capacitors), lump microstrip coupled line power divider (one capacitor), lump-microstrip coupled line power divider (three capacitors) and lump-microstrip ring are designed.

1.2 Aims and Objectives

The main goal of this research is to design, simulate and construct a new microstrip coupled line and ring bandpass filter using lump elements. Meanwhile, power dividers design by applying the same way. These modified design structures has aims to minimizing the total size layout, improving the performance and ease for fabrication.

It is important for the author to understand the fundamental of microwave engineering before designing the filters and power dividers. Parameters of design layouts could be modified easily according to those basic theories.

There are a lot of related journals or articles which can be explored through IEEE Xplore database under the Universiti Tunku Abdul Rahman (UTAR) OPAC system. The author will be able to understand filter better after literature review.

The proposed idea is to design the microstrip filters and power divider with lump elements. Currently, this is the latest technique in the world which reduce total layout of filters without decreases the filter performance. The value of lump-elements will determine the range of frequencies and the strength of the signal. It is aiming to produce wideband that resonates within frequency range from 1 GHz to 5 GHz.

Meanwhile, the microstrip power dividers are the further research from the combination of two microstrip coupled line filters that employed the same lump element technique with different values. The aim is to produce a one input to two output power divider that has an excellent wide bandpass response.

The author is able to design filters and power dividers by using the HFSS version 8 software. Apart from theoretical knowledge, there will also be involved in a hands-on operation to construct the microstrip filters and power dividers through effective research methodology to produce excellent prototypes. Furthermore, the author will be able to measure the frequency responses of these prototypes by using the Vector Network Analyzer and compare the measured result with the simulated one.

Students are able to do an analysis of the results and troubleshoot if any problem exists. Lastly, all the research data and analysis will be written in a journal with the intention to publish in international research society.

1.3 Project Motivation

The motivation of the project is to design lump microstrip coupled line filters, lump microstrip ring filter and lump microstrip power dividers that are publishable in the IEEE Xplore journals.

After completing the literature review throughout the journals in IEEE Xplore, knowledge in filter design is widened. Some of the resonating filters may incur high fabrication cost due to the gap issue. Therefore, the goal of this project is to design small size microstrip filters and power dividers using lump elements which the results comparable to those published in IEEE Xplore.

1.4 Research Methodology

The process of designing the microstrip bandpass filter becomes easier and consumes lesser time by using the computer-aided design (CAD) tools. The designers can simulate the microstrip filter before fabricated it. CAD tools provide precise design with less iteration and design resource costs include those for design, tuning, fabrication and testing can be minimized.

There are three main stages in designing proposed design: simulation stage, fabrication stage and experiment stage. HFSS is chosen to be used in this project due to the accuracy of the software. Few tutorials have been going through to ensure author familiar with the software and hand-on experience on features consist in the software. The tutorials are easy to understand which entitled "*Ansoft HFSS Training Example: Aperture-Coupled Patch Antenna*" and "*Ansoft HFSS Software Demonstration Example: Microstrip Transmission Line*".

In this project TX Line 2003 has been used due to simplicity and accuracy of the software. According to TX Line 2003, the width of a 50 ohm feed line on FR4_eproxy substrate with dielectric constant of 4.4 and thicknesses of 1.57 mm is 3.1 mm.

In the other hand, AWR software is used to model the physical structure of the projects while it's result compare with the HFSS result. The AWR Design Environment comprises two powerful tools that can be used together to create an integrated system and RF design environment: Visual System Simulator (VSS) and Microwave Office (MWO). The tool used in the simulation work is the MWO. It has many functions and main tools.

Microwave Office enables the design of circuits either in schematics or its layout configuration. It can also tune or optimize the designs. The changes are automatic and immediately reflected in the layout. HFSS simulation duration is dependent on the complexity of the design and the computer processing speed. The filter optimisation process consumed a lot of time and it required hard work and commitment in order to finish the tasks. Hence, the MWO simulation is much more efficient than HFSS simulation.

Next will be the fabrication stage. During fabrication, the filter designs have to be printed on tracing paper first before printed on the board. The size of filter must be 100% exact size of the simulation filter design. In order to print out the pattern on the tracing paper, the proposed bandpass filter configuration has to be drawn with CST software because HFSS does not support printing function.

The mask accuracy is very important due to the multilayer coupling technique that required the excellent matching between the top and bottom layer. This is to ensure the proposed filter design in HFSS can be fabricated successfully because the measured result can be easily affected.

Etching is a critically important process module, and every board undergoes etching step before it is complete fabricated. In this project, the wet etching technique is used and it required the board to be immersed in the chemical solution to etch away the unwanted area. The etching steps have to be performed with patient and care because the frequency response of the filter will affected if the unwanted part is not etched away completely.

Finally, the experiment stage is to perform experimental measurement on the frequency response of the fabricated filter. The machine used to measure the experiment result is Rohde & Schwarz ZVB8 Vector Network Analyser (VNA) which shown in figure 1.1. There are some procedures to follow before using the VNA to measure the filter. In the beginning, the author is required to complete a calibration process before starting the measurement.

Figure 1.1: Rohde & Schwarz ZVB8 Vector Network Analyzer (VNA)

The main purpose of the calibration process is to eliminate the effect of signal loss and phase shift introduced by the cable during measurement. The author needs to connect the cable from the two ports of VNA with the calibration kit independently in this process.

In the calibration kit, there are four calibration tools which are named OPEN, SHORT, MATCH and THROUGH. These tools are connected to the cable to perform the calibration through the VNA which is shown on figure 1.4.

Figure 1.2: Rohde & Schwarz Tool Kit

The measurement can be started after the calibration process. The author is required to connect the two cables attached to the VNA with the fabricated filter ports in order to measuring the experiment result. The setting of the frequency ranges and sweep points used to measured have to be the same as the simulated result so that similar measured result with the simulated result can be obtained and compared.

In this stage, the error might be caused by improper etching and pattern transfer process. The author might need to re-fabricate a board in order to obtain the measured result which is similar with the simulated result. The experiment results have been recorded and further discussed in following chapters.

1.5 Thesis Overview

The aims and project motivations have clearly stated in Chapter 1. Research methodology is describes the work flow of the project. It is concluded whole progress of the research which involving simulation, fabrication and experiment stage. A briefly discussion of the method about the simulation tools have been done, fabrication stage have been experienced and how measurement goes on.

The literature review in Chapter 2 is intended to be an introduction and a review of fundamental microstrip filter. It then proceeds with discussion of the coupled lines, microstrip power divider and microstrip ring, followed by description of their recent development. The design considerations and issues also is one of the subtopic which being concerned.

Chapter 3 illustrates the used measurement procedure and results of lump coupled line filters and ring filter.

Chapter 4 illustrates the used measurement procedure and results of coupled line power dividers.

Finally, Chapter 5 concludes this dissertation with a discussion of project results and description of possible future work.

.

CHAPTER 2

LITERATURE REVIEW

2.1 Microstrip Lines

2.1.1 Theory

Microstrip can be fabricated using printed circuit board (PCB) technology and is used to convey microwave frequency signals. It can mount all the active components on top of the board unlike stripline. Hence it is a convenient form of transmission line structure for probe measurement of voltage, current, and waves. Moreover, microstrip is much cheaper than coplanar waveguide as it is lighter and more compact.

Microstrip can be used to design antennas, couplers, filters, power dividers and etc. Since it is not enclosed as a waveguide, it is susceptible to crosstalk and unintentional radiation. However, microstrip has disadvantages which generally lower power handling capacity and higher losses. External shield may be needed for circuits that require higher isolation such as switches.

A conducting strip (microstrip line) with a width *w* and a thickness *t* is on the top of a dielectric substrate that has a relative dielectric constant ε_r and a height *h*, and the bottom of the substrate is a ground (conducting) plane. The general structure of a microstrip is illustrated in Figure 2.1.

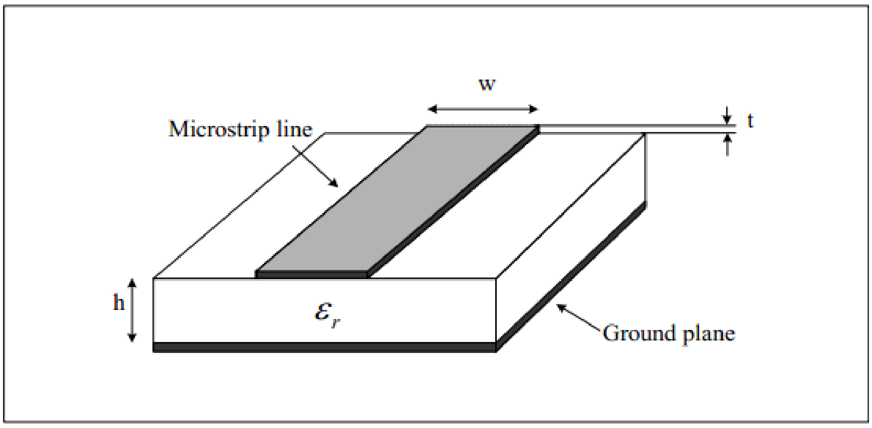

Figure 2.1: General microstrip structure

2.1.2 Design Considerations and Issues

In this project, microstrip line is chosen for this project because it can designs in various patterns depending on the designers' requirements. Author has put a lot of effort on coupled transmission lines, ring filter and power dividers. Further discussions on these microstrip designs will be included in Chapter 2.2 onwards.

The fields in the microstrip extend within two media-air above and dielectric below so that the structure is inhomogeneous. Microstrip does not support a pure TEM wave due to this inhomogeneous nature. With the presence of the two different guided-wave media which are the dielectric substrate (ε_0=3.38) and the air (ε_0=1), it leads to the existence of effective dielectric constant.

Effective dielectric constant is just like is an equivalent dielectric constant of an equivalent homogeneous medium. The maximum value of the effective dielectric constant is affected by the width of microstrip line.

Higher value of effective dielectric constant with wider transmission line because nearly all of the electric field lines will be concentrated between the metal planes in a wide microstrip line. Lesser effective dielectric constant will be obtained in the narrower transmission line.

Description of formulas shown in 2.1a:

Wide transmission line	: Maximum $\varepsilon_{eff} = \varepsilon_r$	
Narrow transmission line	: Minimum $\varepsilon_{eff} = 0.5(\varepsilon_r + 1)$	
Range between	: $0.5(\varepsilon_r + 1) \leq \varepsilon_{eff} \leq \varepsilon_r$	(2.1a)

According to Constantine A. Balanis, the effective dielectric constant can be calculated by using formulas below where *w* represents width of strip, *h* represents height of the substrate and ε_r represents dielectric constant of the substrate. Noted that, there are different solutions for cases which shown in equations 2.1b below:

The $\left(\frac{w}{h}\right)$ stated is the ratio of the width to the height of the microstrip line.

For $\frac{w}{h} < 1$; $$\varepsilon_{re} = \frac{\varepsilon_r + 1}{2} + \frac{\varepsilon_r - 1}{2}\left\{\left(1 + 12\frac{h}{w}\right)^{-0.5} + 0.04\left(1 - \frac{w}{h}\right)^2\right\}$$

For $\frac{w}{h} \geq 1$; $$\varepsilon_{re} = \frac{\varepsilon_r + 1}{2} + \frac{\varepsilon_r - 1}{2}\left(1 + 12\frac{h}{w}\right)^{-0.5}$$

(2.1b)

HFSS version 8 software has considered the effective dielectric factor inside the simulation process which will automatically convert the substrate dielectric constant into effective dielectric constant during the simulation process in order to obtain optimal practical result. Hence, the effective dielectric constant problem will not arise in this program‘s simulations.

Yet, transmission characteristics of microstrips are also described by characteristic impedance Z_0. Characteristic impedance is the ratio of the amplitudes of a single pair of voltage and current waves propagating along the microstrip line in the absence of reflections. The general expression for the characteristic impedance is as shown 2.1c below:

$$Z_0 = \sqrt{\frac{R + j\omega L}{G + j\omega C}}$$

(2.1c)

where R is the resistance per unit length, L is the inductance per unit length, G is the conductance of the dielectric per unit length, C is the capacitance per unit length, j is the imaginary unit and ω is the angular frequency.

In the microstrip transmission line, the characteristic impedance, Z_0 is also a function of height (h) and width (w). It has different solution depending of the ratio of w and h. Nevertheless, effective dielectric constant effect on the characteristic impedance maybe included. According to Bahl and Trivedi, characteristic impedance of microstrip transmission line can be calculated using equation 2.1d:

For $\left(\frac{w}{h}\right) < 1$;

$$Z_0 = \frac{60}{\sqrt{\varepsilon_{eff}}} \ln\left(8\frac{h}{w} + 0.25\frac{w}{h}\right) (ohms)$$

For $\left(\frac{w}{h}\right) \geq 1$;

$$Z_0 = \frac{120\pi}{\sqrt{\varepsilon_{eff}} \times \left[\frac{w}{h} + 1.393 + \frac{2}{3}\ln\left(\frac{w}{h} + 1.444\right)\right]}$$

(2.1d)

In fact, the value of Z_0 is very important because it will affect the reflection loss, S_{11} which is the loss of signal power resulting from the reflection caused at a discontinuity in a transmission line.

Equation of S_{11} described in 2.1e.

$$S_{11} = \frac{Z_{in} - Z_0}{Z_{in} + Z_0} \tag{2.1e}$$

In this experiment stage, the input impedance will be the Vector Network Analyzer (VNA) connector input impedance. Most of the input ports are designed at 50ohm. In order to prevent any reflections, the Z_0 of microstrip lines should be designed as 50ohm accurately and can be controlled by modifying the w, h and ε_{eff} using equation in 2.1d. Thus substrate has constant value of ε_{eff} and h(height), the only variable is the width of the microstrip line.

The author has substituted different value of W in order to obtain the Z_0 value as 50ohm using equation 2.1d. Due to complexity of the equation, it is time consuming for the calculation for different substrate. Fortunately, an user-friendly software, TX Line 2003 is able to calculate the width of the microstrip lines by entering the desire characteristic impedance, height of the substrate and dielectric constant of the substrate.

2.2 Microstrip Coupled Lines

2.2.1 Theory

Coupled microstrip lines are widely used for implementing microstrip filters. Figure 2.3 illustrates the cross section of a pair of coupled microstrip lines under consideration in this section, where the two microstrip lines of width w are in the parallel coupled configuration with a separation s.

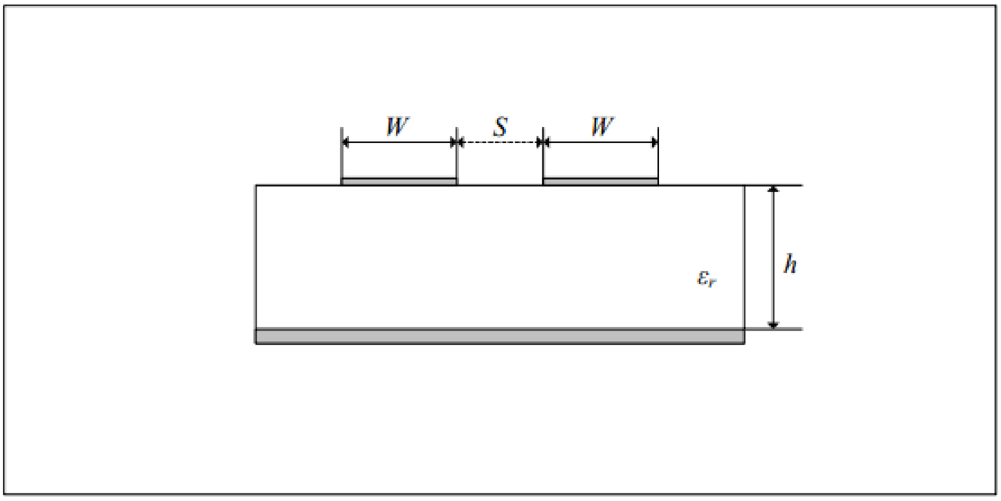

Figure 2.2: Cross section of coupled microstrip lines

This coupled-line structure supports two quasi-TEM modes, which is the even mode and the odd mode. For an even-mode excitation, both microstrip lines have the same voltage potentials or carry the same sign charges, say the positive ones, resulting in a magnetic wall at the symmetry plane, as figure 2.3 shows:

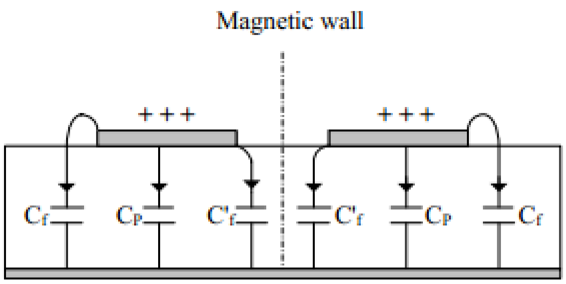

Figure 2.3: Quasi-TEM even-mode of a pair of coupled microstrip lines

In the case where an odd mode is excited, both microstrip lines have the opposite voltage potentials or carry the opposite sign charges, so that the symmetric plane is an electric wall, as indicated in figure 2.4.

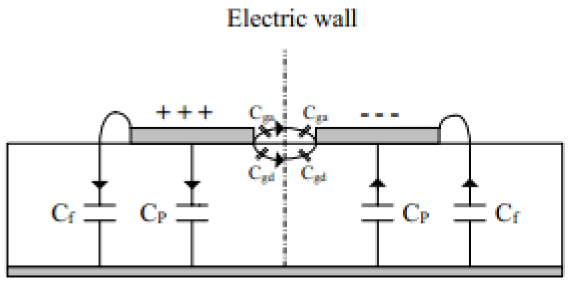

Figure 2.4: Quasi-TEM odd-mode of a pair of coupled microstrip lines

In general, these two modes will be excited at the same time. However, they propagate with different phase velocities because they are not pure TEM modes, which mean that they experience different permittivity. Therefore, the coupled microstrip lines are characterized by the characteristic impedances as well as the effective dielectric constants for the two modes.

2.2.2 Recent Developments

2.2.2.1 1.7GHz Coupled-line Bandpass Filter

The author has reviewed a paper entitled "1.7GHz Coupled-line Bandpass Filter" by Dr Robert Frias. This paper presents a fundamental design of a coupled line bandpass filter at 1.7GHz. The 3rd order Equiripple (Chebyshev) bandpass filter has centre frequency of 1.7GHz and a typical bandwidth of 90MHz. It is mainly intended for use in meteorological satellites (Meteosat, GOES, GOMS) receiving equipment. It can be also used also in point-to-point wireless communication and other RF applications in this band.

Typical passband specifications are stated in the journal clearly. The table shows again in figure 2.5 below.

Center frequency	1.7 GHz
3 dB bandwidth	90 MHz
Insertion loss	> 1.6 dB
Return loss	> 9 dB
Group Delay Variation	5 ns

Figure 2.5: Typical Passband of 1.7GHz coupled line bandpass filter

The coupled line filter structural layout is shown in figure 2.6.

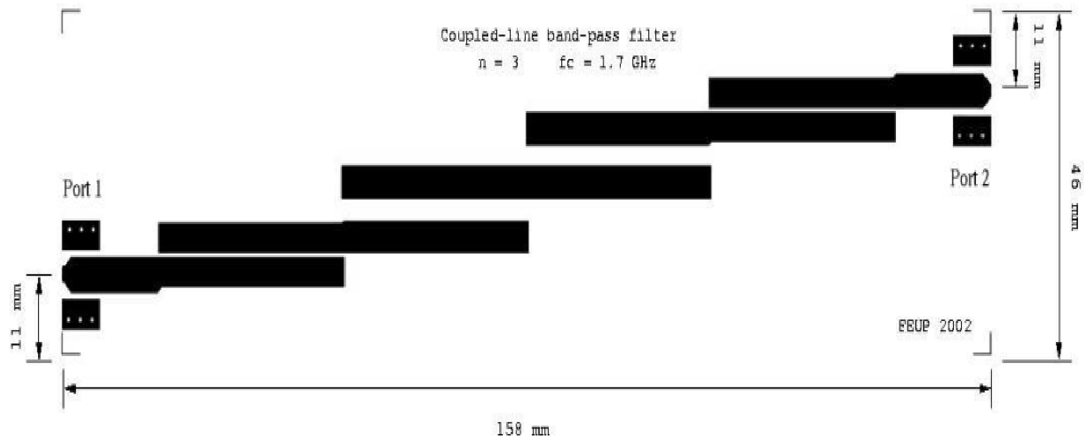

Figure 2.6: Structural layout of 1.7GHz coupled line bandpass filter

The proposed design had 50 ohm impedance through transmission line. Advantage this designed bandpass filter is low cost but it's drawback is the size layout was large which length of 158mm. Figure 2.7 shows the measured performance of particular filter.

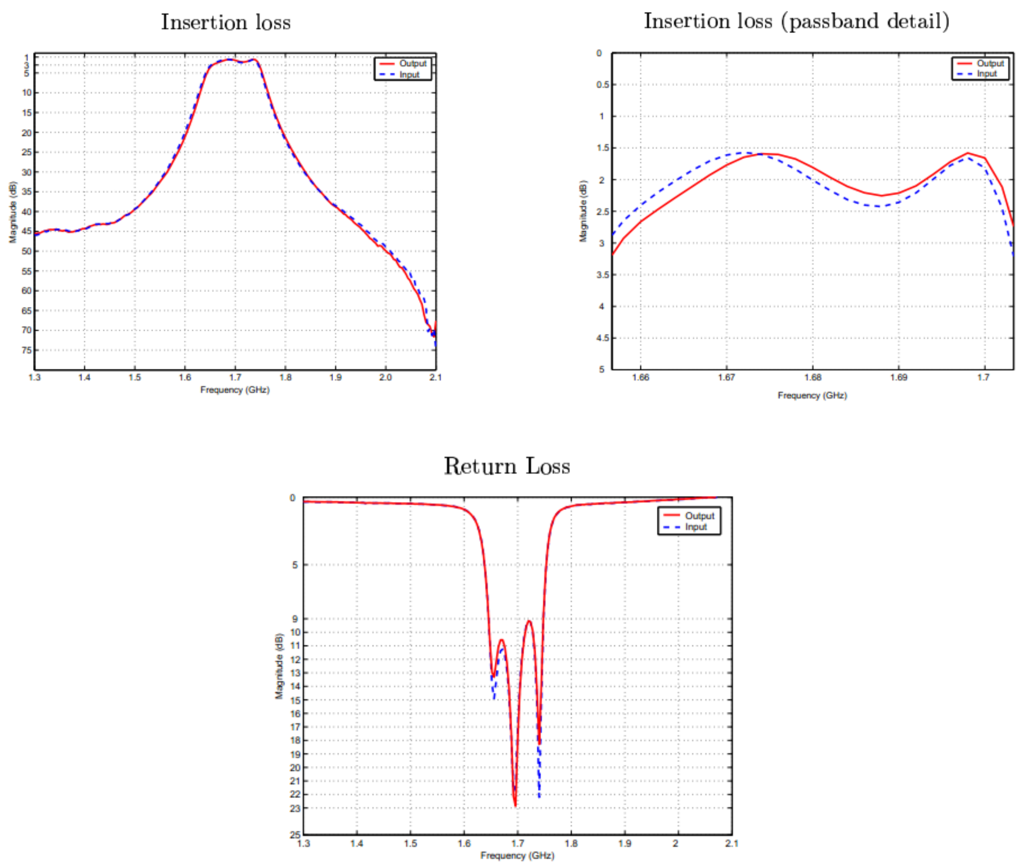

Figure 2.7: Measured performance of coupled line bandpass filter

It can be observed that the frequency response of the bandpass filter has very good selectivity with sharp roll-off at the transition between the passband and reject band.

Lump microstrip coupled line filter which proposed by author was based on this coupled line design. However the length has shorten where replaced by inductors and the gap between lines have replaced by the capacitors. In conclusion, the paper presents the fundamental design of coupled line filter and is a good reference for author in the following proposed designs.

2.2.2.2 A Compact Bandpass Filter Using Lumped Coupling Elements between Input Port and Output Port

A novel compact T-shaped resonator filter using the lumped coupling elements between two ports is studied. The proposed design entitled “A Compact Bandpass Filter Using Lumped Coupling Elements between Input Port and Output Port” by Qing-Xin Chu, Li Fan, and Huan Wang.

The advantages of this new type of filter over conventional ones are that the frequency responses have three transmission Z_{ps}, the bandwidth and transmission Z_{ps} can be independently controllable.

The number and position of some transmission zeros can be controlled by simply varying the values of the lumped coupling elements, the length of short-circuited branch of T-shaped resonator can change the bandwidth of the filter greatly. The theoretical analysis and design procedures have been successfully verified by the experiment.

The circuit model of the proposed filter is shown in fig. 2.8, which consists of a T-shaped resonator and the capacitor between the input port P1 and the output port P2.

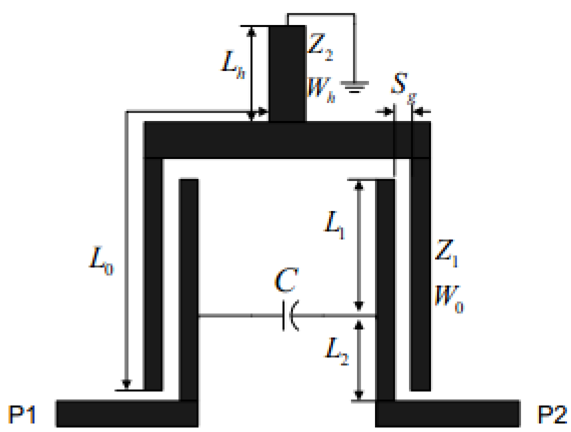

Figure 2.8: Circuit model of a filter using lumped coupling element between input port and output port

The position of the lumped capacitor (L_1 and L_2) can adjust the transmission Z_{ps} greatly. By using the dielectric substrate with relative permittivity of ε_r =2.56 and thickness of 0.775mm, we can obtain the dimension of the filter shown in Fig.2.8, which operates at 3GHz with a fractional bandwidth of about 20% as follows: W_0=0.5mm, L_0=16.4mm, W_h=0.4mm, L_h=1.1mm, L_1=5mm, L_2=7mm.

The multi-paths from input port to output port make it possible for the filter to generate more finite transmission Z_{ps}. The signal from P1 mainly comes into the resonator. Meanwhile, the direct signal path from P1 to P2 is capacitor.

Fig. 2.9 plots the simulated -magnitude of the filter in fig.2.8 under varied capacitance value, i.e., and 0.05 pF, respectively.

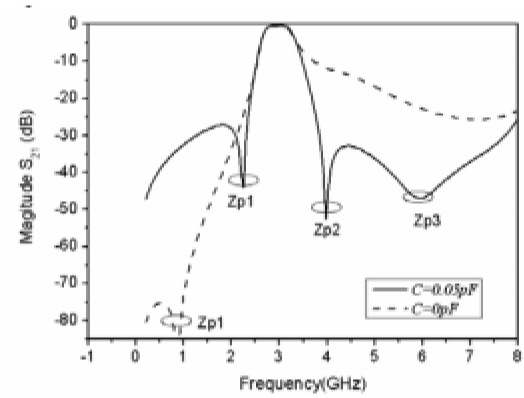

Figure 2.9: Impact of capacitor value in figure 2.8

The frequency response as shown under the case of C=0.05pF (solid line), has good skirt selectivity and more controllable finite transmission zero points (Zp3) compared with the typical filter when C=0pF. It should be noted that the filter gene rates two more transmission Zps due to the capacitor.

For more general applications, the lumped capacitor can be implemented by a coupled gap or coupled transmission lines. In fig. 2.10, the configuration for filter with coupled transmission lines is shown. The series-connected inter-digital capacitor between port P1 and port P2 has four fingers of width of W_c and space of S_c, and the finger length of L_c can be used to achieve varied capacitance density.

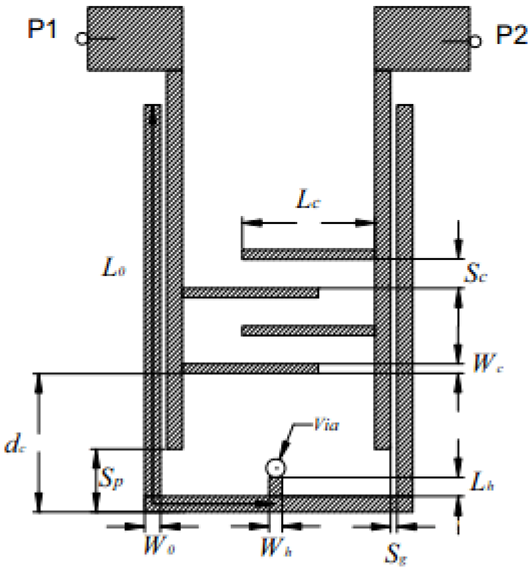

Figure 2.10: Configuration of the filter using lumped coupling elements between input port and output port.

In addition, the position of inter-digital capacitor d_c also is an important factor for the transmission Zps, whose effect will be soon investigated. The distance between I/O feed stubs and the bottom of the filter (S_p) also can influence the transmission Zps.

Then, the study of the novel filter structure shown in Fig. 2.10 will include two parts, one is the transmission Zps for varied position of inter-digital capacitor of d_c, and the other is bandwidth of frequency responses of the filter for varied length of short-circuited branch of L_h. Except for d_c and L_h, all of the physical dimensions for a filter operating at 3GHz in both case are also fixed as follows: W_0=0.5mm, L_0=16.4mm, S_g =0.2mm, S_c=0.9mm, L_c=4.2mm, W_h=0.4mm, S_p=0.8, W_c=0.3mm.

To observe the effects of the position of inter-digital capacitor d_c on the filter responses, the transmission characteristics for different d_c is shown in Fig. 2.11. There is one transmission zero point at the lower stopband and two transmission zero points at the higher stopband when the equivalent capacitance value of the inter digital capacitor is not zero.

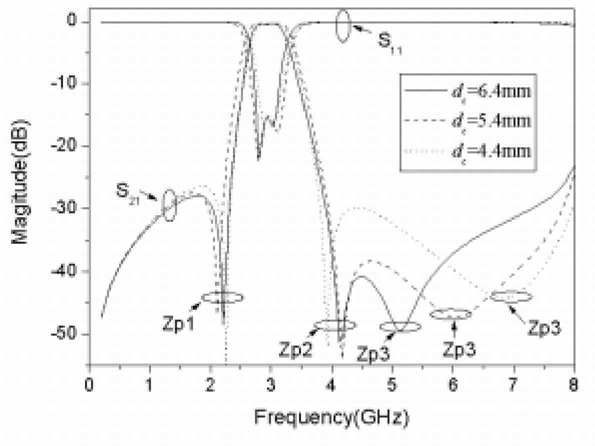

Figure 2.11: Impact of the position of inter-digital capacitor d_c

The inter-digital capacitor and the coupling between resonator and I/O ports make it possible for the filter to generate two finite transmission Zps in the spectrum. The similar frequency response for the first spurious frequency at 3 f_0 (where f_0 is the centre frequency of the filter passband) can generates an additional Zp (as Zp3 in Fig. 2.10) in the upper stopband.

When the value rises from 4.4 mm to 6.4 mm, third of transmission Zp shifts down. These controllable Zps as well as stopband roll off have the advantages of meeting different filter specification requirements and improving rejection at certain interference frequency. It should be noticed that the centre frequency is not changed when the transmission Zp shifts down.

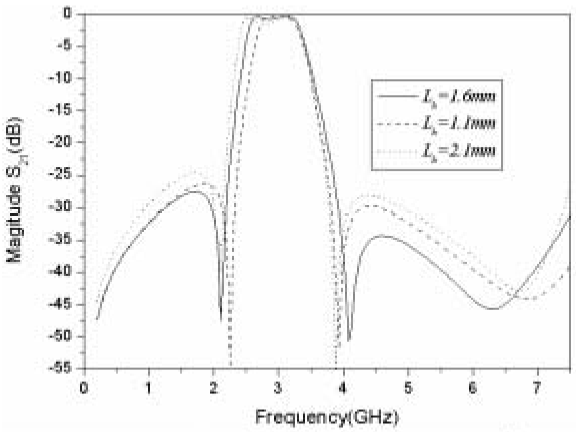

Figure 2.12: Impact of the length short circuited branch L_h

Fig. 2.12 plots the simulated frequency responses of the filter in Fig. 2.10 under varied length of short-circuited branch, i.e., L_h=1.1mm, 1.6mm, and 2.1mm, respectively. It is can be seen that as rises from 1.1mm to 2.1mm, the bandwidth is wider and wider.

This phenomenon attributes to the relation of the f_{even} and the dimension of T-shaped resonator. It is clear that $f_{odd}>f_{even}$, f_{odd} is independent to the length of short-circuited branch L_h .As the short-circuited branch is longer, $f_{even}$is smaller, f_{odd} is not changed. Therefore, the bandwidth increase, and the centre frequency shifts down with the longer short-circuited branch.

The measured specifications of the BPF filter are: operating frequency of 3GHz with 26% bandwidth, insertion loss of 0.7dB, stopband rejection in the ranges of 4.2- 6.3 and 0-2.2 GHz more than 28dB, four Zps(including zero frequency) in the stopband with attenuation over 45dB. Return loss in the passband is less than 15dB. The measured insertion loss of 0.7 dB is greater than that of the simulated one of 0.4dB. The additional losses are mainly from the metal loss and radiation loss.

The filter has good skirt selectivity characteristics as well as stopband rejection. The size is only 16mm x6 mm. The fabricated filter and the simulated and measured frequency response are illustrated in Fig. 2.13. Both simulation and measured results are matched well.

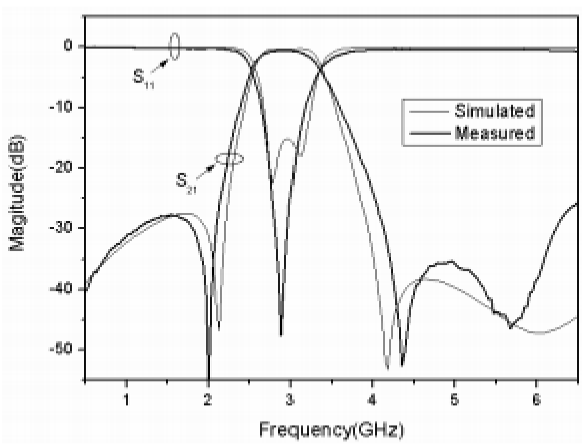

Figure 2.13: Frequency response of presented microstrip filter

In this paper, a new T-shaped resonator filter using inter-digital capacitor between I/O ports to introduce three transmission zeros has been proposed. The inter-digital capacitor and the coupling between resonator and I/O ports generate three transmission zeroes in the stopband. By tuning the position of the inter-digital capacitor, the transmission zero in the upper stopband can be prescribed to obtain desired filter performance.

The bandwidth of the filter also can be changed by adjusting the length of short-circuited branch of T-shaped resonator. The simulated results of the filter, which are in good agreement with experiment, have demonstrated that the novel BPF has compact size, controllable Zps and sharp as well as deep stopband rejection. After study through this paper, author is interest to apply the lumped element for size reduction of the filter as well.

2.3 Microstrip Power Divider

2.3.1 Theory

Power dividers are very important components in microwave and millimetre-wave circuits. In recent years, there has been increasing demand for dual-frequency equipment due to the development of multiband technologies. The simplest power divider circuit has three ports. The behaviour of the circuit can be explains using the scattering parameters. The scattering matrix of is composed of nine components given by:

$$[S] = \begin{bmatrix} S_{11} & S_{12} & S_{13} \\ S_{21} & S_{22} & S_{23} \\ S_{31} & S_{32} & S_{33} \end{bmatrix} \tag{2.3}$$

Wilkinson power divider was proposed by E. J. Wilkinson, as a method of distributing power to attain equal phase and equal amplitude condition. It was based on a coaxial line as the input. The hollow inner conductor is split into 8 splines of λ/4 long, and linked by a shorting plate. The design is depicted in Figure 2.14.

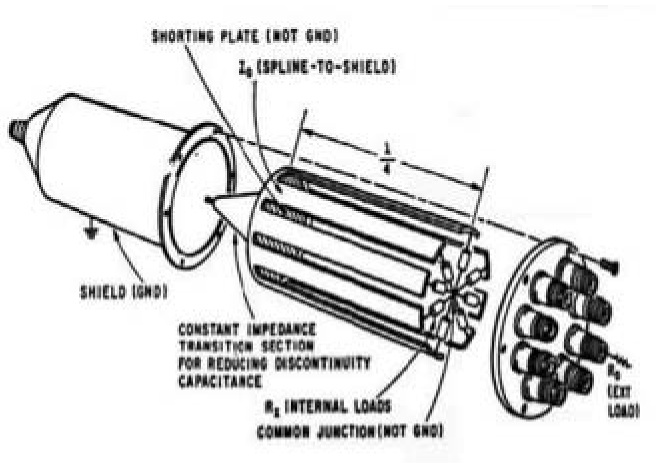

Figure 2.14: Power divider developed by Wilkinson

At the back end of spline, an internal resistor is placed to connect them radially to a common junction. Finally, the output connectors are attached at the end of each spline. It was noted that all splines were designed to be at the same potential when signal is supplied to the input coaxial line and matched loads are connected to the outputs. This idea is indeed amazing because a power divider which is reciprocal, lossless and having matched ports has been proposed. Such properties were never achievable using a T-junction power divider.

A simple power divider cannot simultaneously have all the properties of lossless, reciprocal, and matched. Hence, the Wilkinson power divider was developed. Here, an isolation resistor is placed between the output ports to help achieve the properties. Dissipation of energy occurs only in isolation resistor when signal enters the network from any output port. However, it should not affect Wilkinson network efficiency.

Besides, this isolation resistor provides perfect isolation to protect output ports at the operating frequency. Generally, Wilkinson power divider can have any number of output ports. A basic three port Wilkinson power divider of port characteristic impedance Z_0 is schematically shown in Figure 2.15.

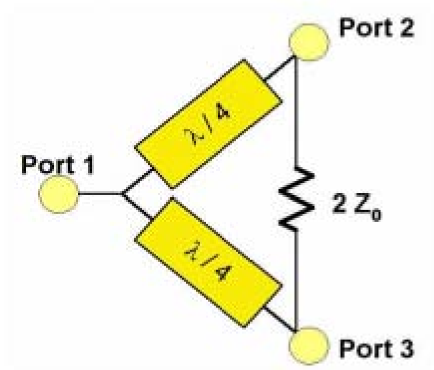

Figure 2.15: Schematic diagram of a Wilkinson power divider

To analyze the Wilkinson network, two approaches are used; the even-mode analysis and the odd-mode analysis. Figure 2.16 shows the simplified equivalent circuit of the power divider.

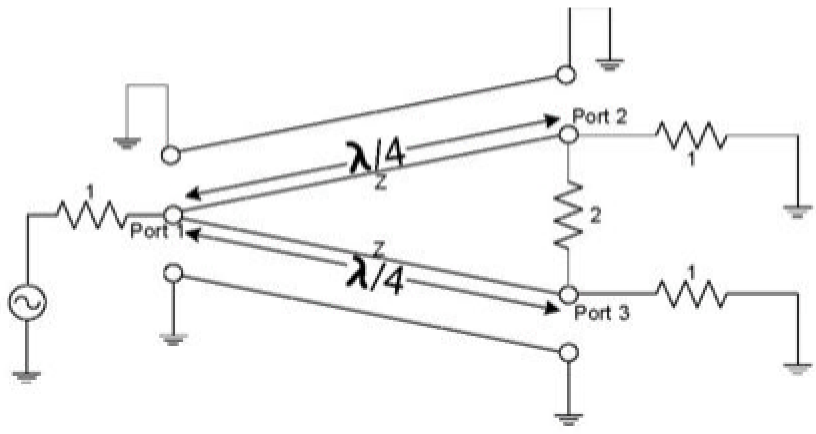

Figure 2.16: Simplified equivalent circuit of the Wilkinson power divider

2.3.2 Recent Developments

2.3.2.1 Coupled Line Power Divider with compact size and bandpass response

The author reviewed P.K. Singh, S. Basu and Y.-H. Wang's paper, entitled "Coupled Line Power Divider with compact size and bandpass response". The proposed divider is equivalent to the series connection of a single-stage coupled line band-pass filter and a conventional Wilkinson divider. Thus, a divider provides the frequency response of a single-stage bandpass filter rather than a wide and fixed bandwidth of the conventional Wilkinson divider with the same quarter wavelength (λ /4) length of the microstrip lines.

In addition, owing to the coupled line structure, the width and spacing of the microstrip lines are reduced, thereby resulting in the miniaturisation of the overall divider width. The proposed dividers were realised on a RO 4003C substrate with thickness h =0.81 mm, dielectric constant ε_r = 3.38 and loss tangent tan δ=0.004. The schematic of the pro-posed coupled line divider is shown in figure 2.17.

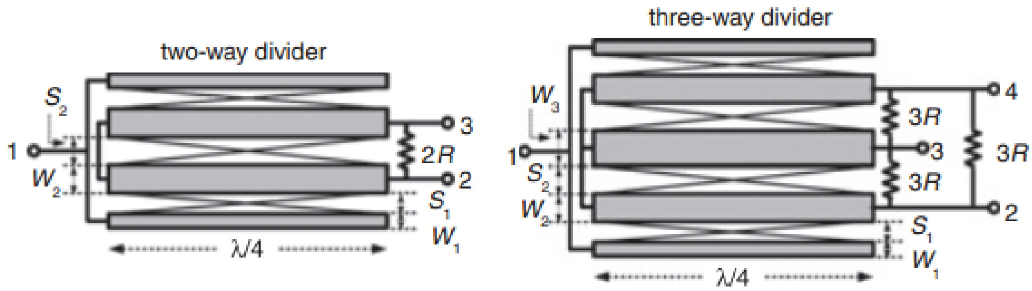

Figure 2.17: Schematics of proposed coupled line dividers

As can be seen, the layout width of the dividers is greatly reduced in the present design. The parameter values for the three-way divider are S_1 =0.2 mm, S_2 = 0.23 mm, W_1= 0.20 mm, W_2= 0.20 mm, and W_3=0.36 mm.

The deviation of some results from the centre frequency is basically due to resistance connections and associated parasitic. The bandwidth of the divider can be controlled by the input coupling gap S_1, likewise single stage coupled line bandpass filter. The results of the two-way and three-way divider are shown in figure 2.18 and figure 2.19.

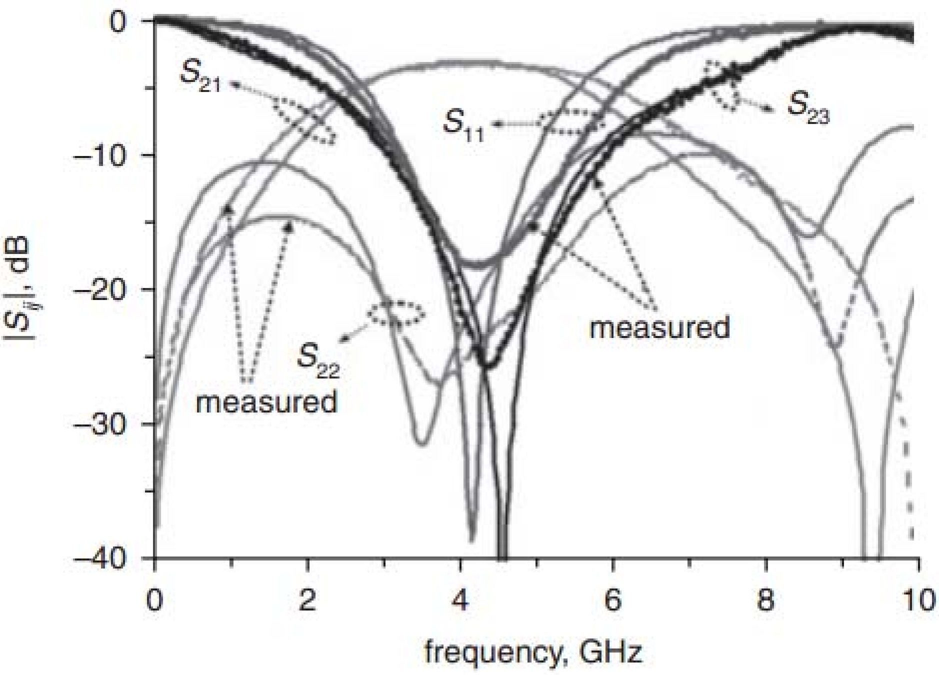

Figure 2.18: Simulated (continuous lines) and measured (dotted lines) two-ways S-parameters

This new power divider using coupled microstrip lines is proposed to improve bandpass frequency response and compact size. The circuit is miniaturised when considered as an integration of a bandpass filter and conventional Wilkinson power divider. This also presents that the power divider can be realised with closely spaced microstrip lines.

The coupled line divider is simple, compact, and ideal for integrated circuit applications. The idea of miniature coupled line power divider design inspired author the creation of coupled line bandpass filter using lumped element which discuss later.

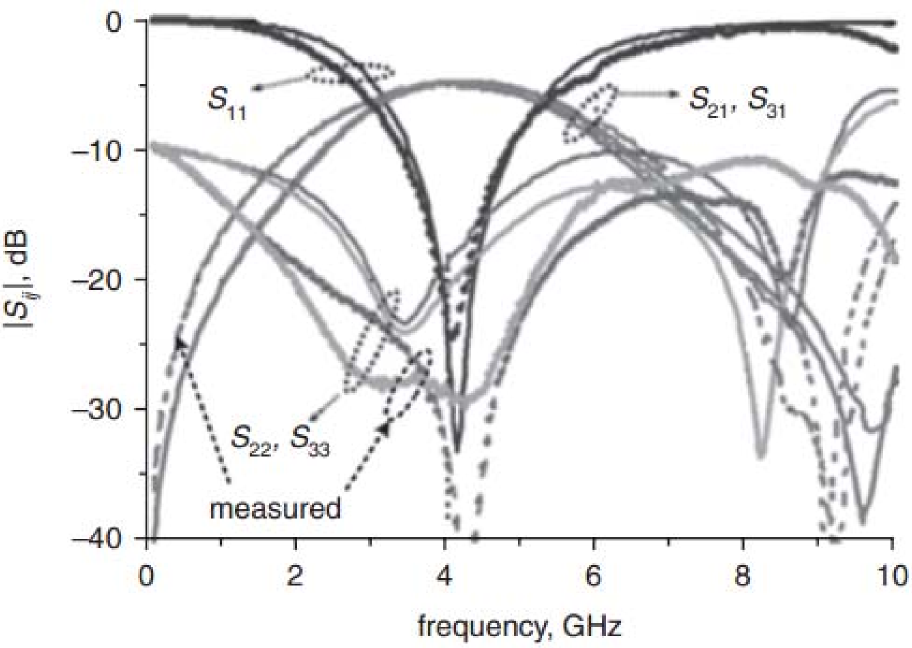

Figure 2.19: Simulated (continuous lines) and measured (dotted lines) three-ways S-parameters

2.3.2.2 Multilayer Unequal Microstrip Power Divider

Meanwhile, multilayer coupling technique is also employed in a paper entitled "Multilayer unequal Microstrip Power divider" by Sheikh S.I. Mitu, SMIEEE, FIET and Sulaiman L. Taiwo. This paper presents a design of a C-band multilayer aperture coupled microstrip power divider.

In the introduction part, authors in this paper mentions that Wilkinson power divider is widely applied in the power divider designed due to its simplicity and high isolation between output ports. However there is a big problem if it is applied in power splitter which needs high impedance of microstrip line. So authors introduce the defected ground structure in the design and it will improve the aspect ratio (W/H).

Figure 2.20 shows top view of the compact aperture coupled two-way microstrip power divider proposed. For the power divider proposed, the dimensions used are: L_a = 8.25 mm, L_b= 10mm, W_p= 4.5mm, Ws = 3mm, L_s = 17.7mm, W_{ms} =3.04 mm, g = 4.9mm and t = 1mm. The substrate height is 1mm and the dielectric constant is 2.6. 3D structure of the design is shown in figure 2.21

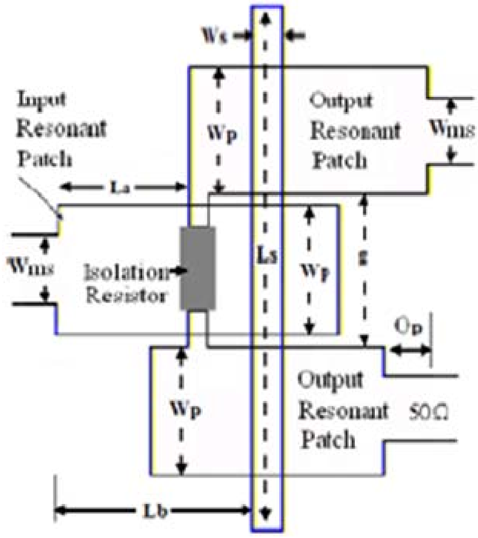

Figure 2.20: Top View of the power divider

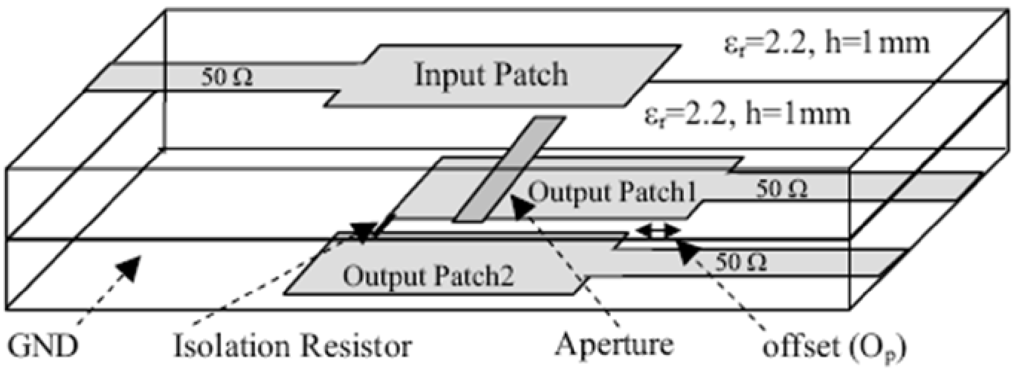

Figure 2.21: 3D-view of the power divider

The simulated and experiment results has low insertion loss, high isolation between the output ports and large impedance bandwidth. Moreover, the experiment results agreed well with the simulated result of the power divider in figure 2.22.

A compact aperture coupled microstrip power divider for unequal, but in-phase, power split presented. The authors of this paper concluded that the response of the device is improved by optimizing the patch and aperture dimension and positions [9]. After reviewed some research paper on this slot resonator design, these ideas will be employed for the development of slot resonator for the new bandpass filter and power divider in this research project.

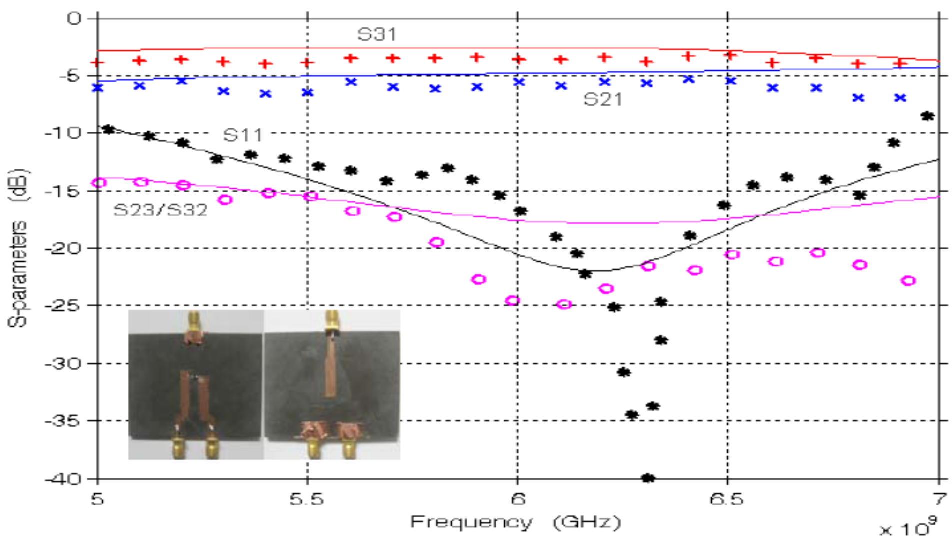

Figure 2.22: Simulated and experimental reflection (S_{11}), transmission (S_{21}, S_{31}) and isolation (S_{23} and S_{32}) responses of the power divider

2.4 Microstrip Ring

2.4.1 Theory

Conducting patch antennas are the most commonly used microstrip antennas. Another two extreme cases are the printed patch and the printed loop antennas, as shown in figure 2.23.

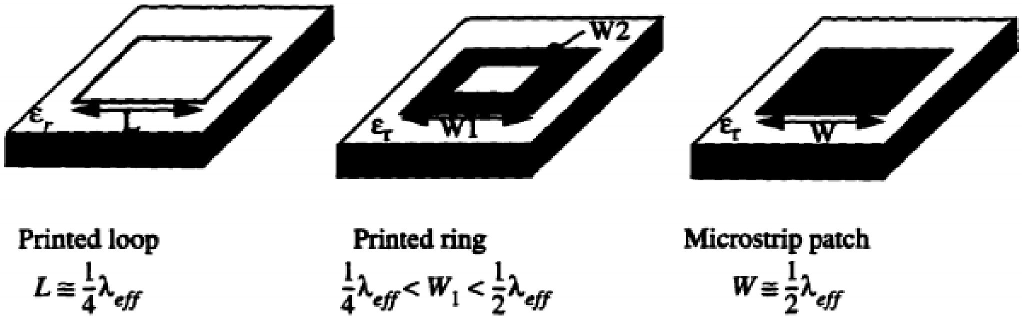

Figure 2.23: Geometry of printed loop, ring and microstrip antennas

In spite of their relatively similar geometry, their electrical behaviour is quite different. The printed patch behaves as a one-dimensional resonator, and thus its width W, at resonance, is about a half wavelength, 1/2 λ_{eff} .

On the other hand, the printed loop behaves as a shorted ring, and thus resonates when its circumference is about a multiple of the substrate effective wavelength and each side length L becomes about a quarter wavelength, 1/4 λ_{eff}. It is therefore half the size of the printed patch antenna. The loop is a relatively narrow band antenna.

The intermediate configuration is a printed ring antenna, which is similar to the patch, except its central conducting portion of width W_2, is removed. This width W_2, provides a new parameter to control its resonance and impedance. Perforated microstrip patches have been used previously to allow dual frequency operations. Their performance, however, has not been investigated adequately.

2.4.2 Recent Developments

2.4.2.1 Novel Miniaturized Open-Square-Loop Resonator with Inner Split Rings Loading

From the paper of Ban-Leong Ooi and Ying Wang, the adoption of flower rings coupled with inner split rings within an open-square-loop resonator for size miniaturization is first analyzed and designed.

In this paper, instead of using lumped-element components or adding a mixed dielectric to the design, which will eventually increase the overall cost of production, an alternate way of producing a size reduction of an open-loop squared resonator is explored as figure 2.24 below.

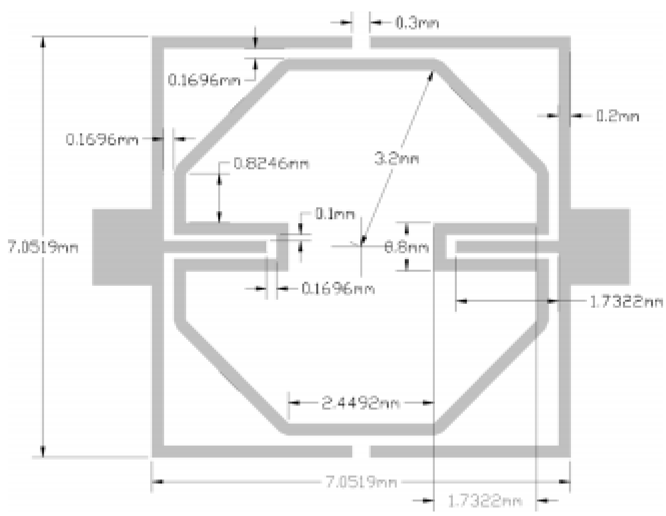

Figure 2.24: Preliminary Structure

Figure 2.24 above illustrates a new open-loop squared resonator that differs greatly from that proposed by the authors. As noted from this figure, this preliminary structure has folded dual rings that help to increase the internal magnetic coupling. The line width of the dual-ring open-loop resonator corresponds to 100ohm at the designed frequency of 4.75 GHz.

The proposed preliminary structure is simulated with a dielectric permittivity of 10.2 and a thickness of 1.27 mm. The simulated response of the structure is given in Fig. 2.25.

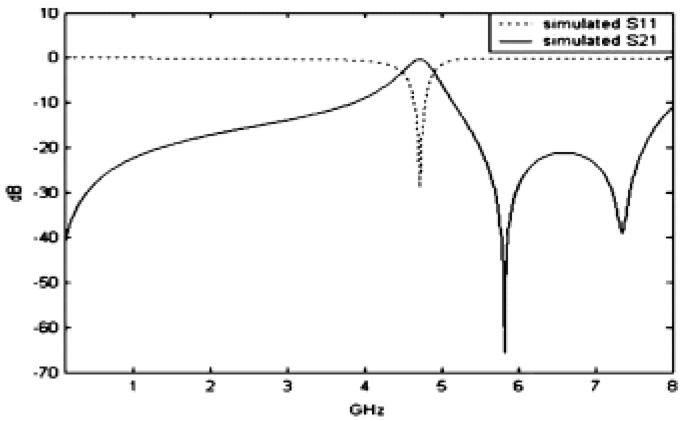

Figure 2.25: Simulated responses of the preliminary structure

To fully understand the principle behind this preliminary structure, the equivalent circuit, as shown in fig. 2.26, is adopted for the analysis. For ease of analysis, we assume that the preliminary structure is lossless. With equal polarity at both the input and output ports, there exists an open-circuit plane along the vertical symmetry plane of the structure. Similarly, with opposite polarity at both the input and output ports, there exists a short-circuit plane along the vertical symmetry plane of the structure.

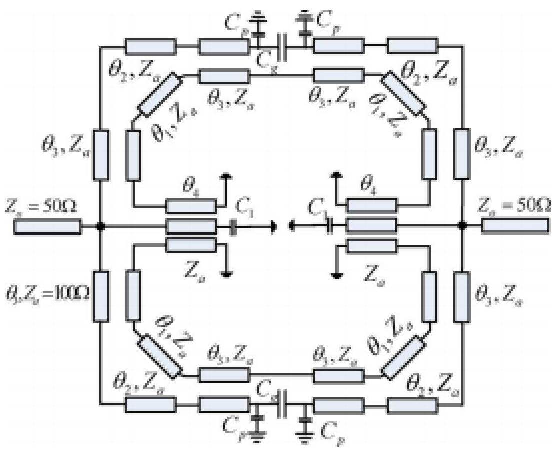

Figure 2.26: Equivalent circuit of the preliminary structure

A novel technique of miniaturizing the open-square-loop resonator has been proposed. By designing the proposed resonator at a higher frequency followed by the insertion of multiple inner split rings, a resonator with 2.94% smaller area, as compared to the loop resonator, and 5.5% smaller area, as compared to the hairpin resonator, is achieved. A loading factor of 48.4% for the resonator has been achieved.

To further demonstrate the method, a novel dual-mode open-loop resonator operating at 2.5 GHz was then designed. Close and good agreement between the measured and simulated results has been achieved. Author may learn from the equivalent circuit in figure 2.26 above which method of inserting those lump elements using AWR software.

2.4.2.2 Compact Microstrip Square-Loop Dual-Mode Bandpass Filter Design with Wideband Response

Meanwhile, multilayer coupling technique is also employed in a paper entitled “Compact Microstrip Square-Loop Dual-Mode Bandpass Filter Design with Wideband Response” by Ting-Shan Lv, Si-Weng Fok, Pedro Cheong, and Kam-Weng Tam. This paper presents a design of a dual-mode bandpass filter using square-loop resonator is proposed for wideband applications.

As the structure is shown in fig. 2.27, the conventional input and output ports with direct coupling feed lines are modified to tight coupling feed lines in this structure.

The simulation and the experimental implementation are carried on an RO4003 substrate with relative dielectric constant ε_r = 3.38 and thickness d = 1.524 mm.

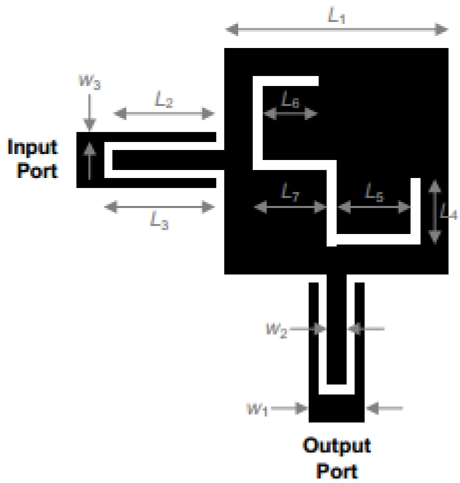

Figure 2.27: Proposed Structure with Direct Coupling

From Fig. 2.28, the fractional bandwidth of both the simulation and experimental is computed as 74%, and the proposed filter offers a good matching of 10 dB and the insertion loss is less than 0.8 dB when simulation.

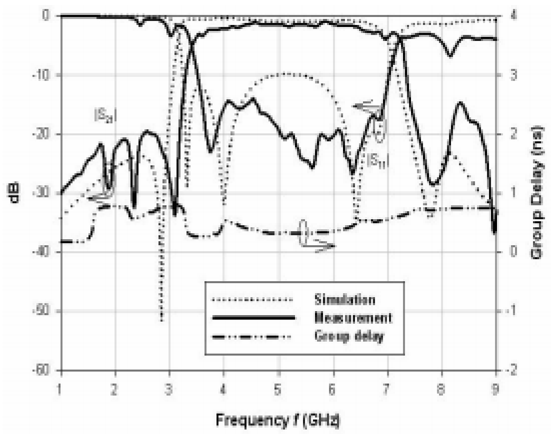

Figure 2.28 : Comparison of simulated and measured passband

Two transmission zeros at the lower and upper sideband are noted at 2.85 GHz and 7.81 GHz respectively. The attenuation outside the passband remains under 20 dB. The matching is better than 14 dB and the maximum insertion loss is measured as 1.2 dB within the passband.

A slight shifting of the transmission zeros along the sideband is observed but the shifting is no more than 0.23 GHz with the two transmission zeros recorded at 3.08 GHz and 7.83 GHz. The simulation and measurement results are in good agreement.

A wideband filter using square-loop dual-mode bandpass filter is proposed and designed for wide bandwidth in UWB application. The structure is based on a one-wavelength square ring resonator and stepped impedance resonator with and without capacitive termination attached to two inner arms of the square ring resonator. It is reported that a fractional bandwidth of 74% and insertion loss is less than 1.2 dB. A flat group delay of less than 1ns is measured in the passband.

From this paper, author realizes a wideband bandpass response as the main goal. This bandpass structure takes full advantage of the capacitive loading effect for wideband response while the tight coupling feed line is beneficial in significant attenuation improvement.

Hence, this paper is a good reference which as a foundation of capacitive loading effect. It has motivated author to propose a square ring which achieve good performance with lump element.

CHAPTER 3

FILTER

3.1 LUMP MICROSTRIP COUPLED LINE FILTER (1 CAPACITOR)

3.1.1 Configuration

A lumped microstrip coupled line bandpass filter with 1 capacitor design pattern is proposed. All description of the proposed filter configuration has been listed in Figure 3.1.

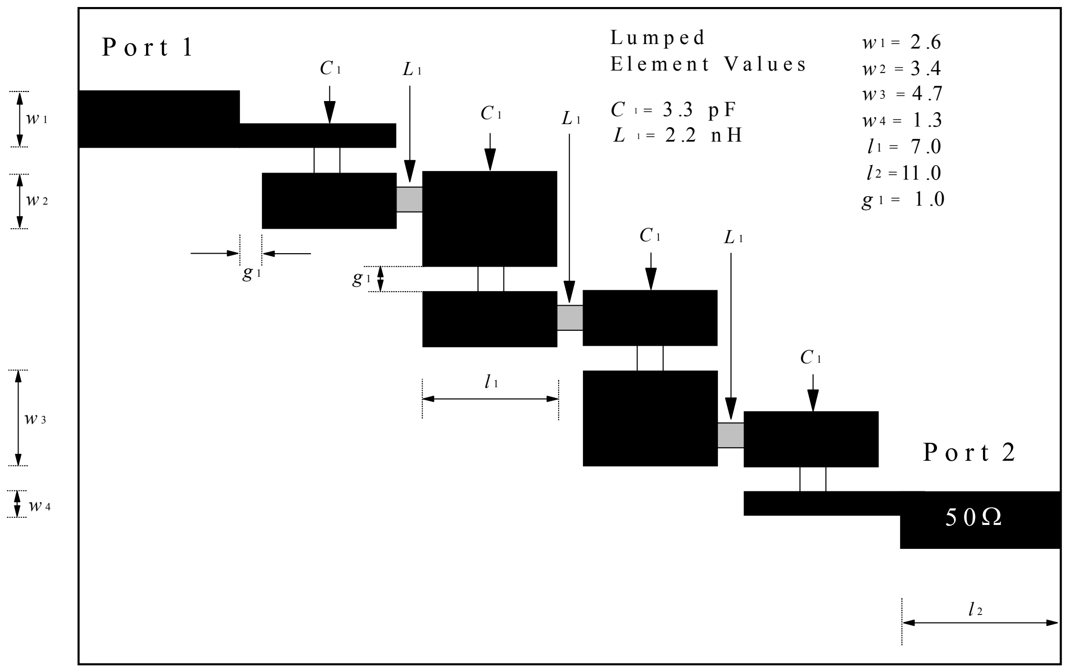

Figure 3.1: Top view of lump microstrip coupled line filter with 1 capacitor

A FR_4 epoxy substrate of relative permittivity, ε_r = 4.40 and thickness, h = 1.57 mm was used in this microstrip bandpass filter design. The dimension of the bandpass filter is 67 x 55mm^2. Parameters of the band-pass filter: l_1 =7 mm, l_2 =11 mm, g_2 =1 mm, w_1 =2.6 mm, w_2 =3.4 mm, w_3 =4.7 mm, w_4 =1.3 mm. Capacitors value of C_1 is equal to 3.3pF. Inductor value of L_1 is equal to 2.2nH.

3.1.2 Transmission Line Model

The same design pattern has been defined using Advanced Wireless Revolution (AWR) software modelling as the result reference. Equivalent circuit is shown in figure 3.2.

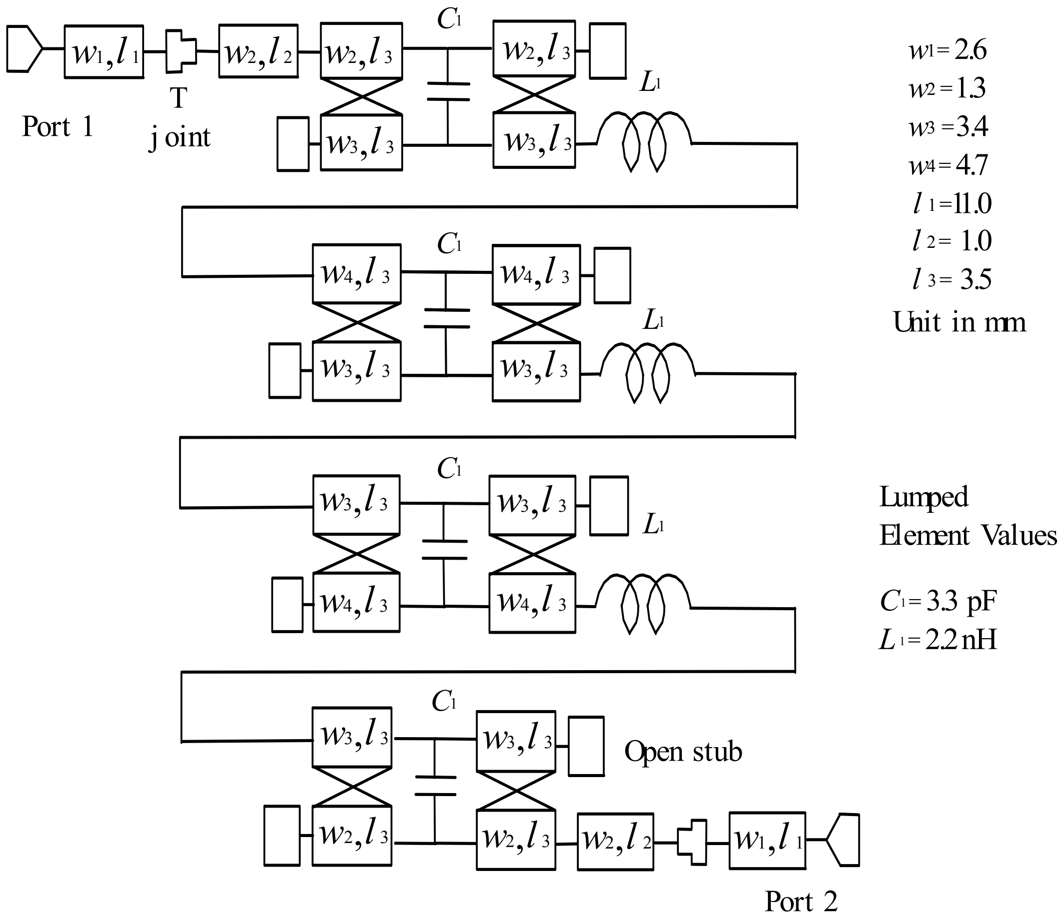

Figure 3.2 Equivalent circuit of lump microstrip coupled line filter with 1 capacitor

3.1.3 Results and Discussion

The results are measured by Rohde & Schwarz Vector Network Analyzer ZVB8 (VNA) and simulation results are plotted with Freelance Graphic suite software as in figure 3.3. In fact there are two simulation results, which simulated by different software, HFSS and AWR. The measured result is verified well with the simulated results. The comparison between the measured result and the simulation results of lumped coupled line microstrip filter with 1 capacitor is shown in Figure 3.3.

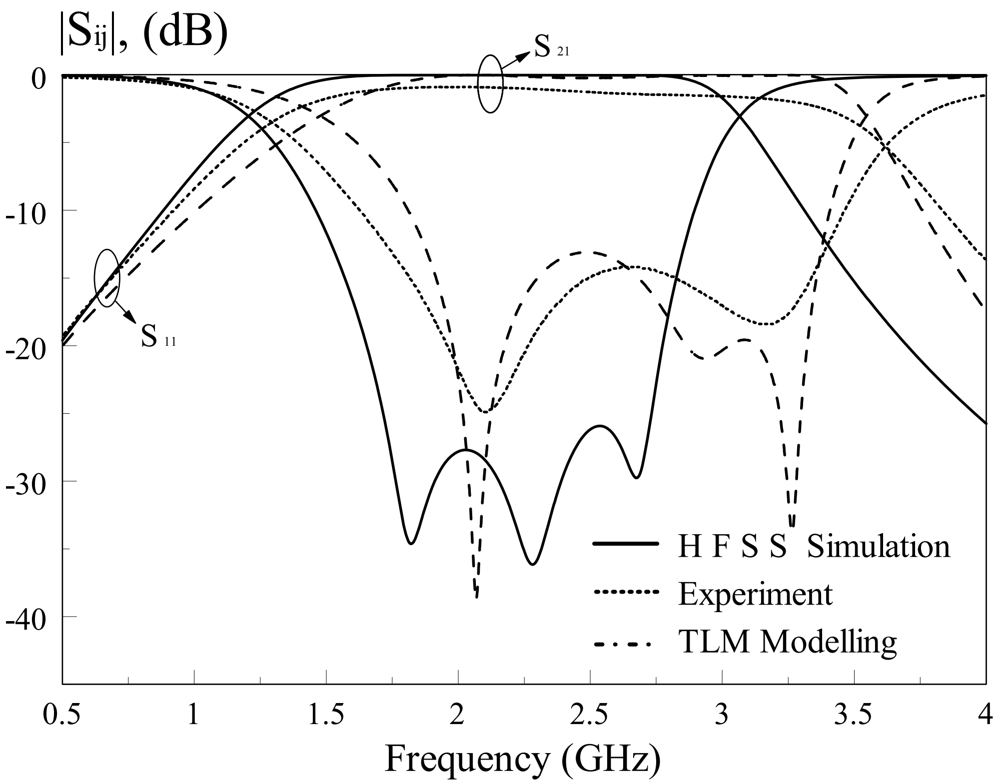

Figure 3.3: Measured and simulated S_{11} and S_{21} of lump microstrip coupled line filter with 1 capacitor

Figure 3.3 presents that the proposed filter is resonates from 1.26 GHz to 3.53 GHz. It has wide passband and low insertion loss. The formulas to calculate the center frequency, bandwidth and error are as table 3.1 below. Center frequency of a filter is the measurement between the upper and lower cutoff frequencies. Meanwhile, bandwidth is the difference between the upper and lower frequencies in a contiguous set of frequencies. Sometimes, it is referred as passband bandwidth.

Table 3.1: Formulas Table

Center Frequency =

$$\frac{(\text{Lowest Frequency}, f_c) + (\text{Highest frequency}, f_H)}{2}$$

Bandwidth =

$$\frac{(\text{Highest frequency}, f_H) - (\text{Lowest Frequency}, f_L)}{(\text{Centre Frequency}, f_C)} \times 100\%$$

Error =

$$\frac{|(f_C(\text{measured}) - (f_C(\text{simulated})|}{(f_C(\text{measured})} \times 100\%$$

The center frequency (f_c), bandwidth and error between measured and simulated results were calculated. The results are shown in table 3.2.

Table 3.2: Comparison Results Table

	HFSS Simulated	Measured	AWR Simulated
Minimum Insertion Loss (dB)	-0.019	-0.902	-0.021
3-dB reference (dB)	-3.019	-3.902	-3.021
f_L (GHz) / f_H (GHz)	1.21/3.06	1.26/ 3.53	1.48/3.54
f_c (GHz)	2.14	2.40	2.51
Bandwidth (%)	86.65	94.78	81.90
Error (%)	10.86	-	4.58

The measured center frequency is 2.40 GHz, which is very close to the HFSS simulated value of 2.14 GHz (error 10.86 %) and AWR value of 2.51 (error 4.58%).

With reference to the result, the measured result verifies well with the simulated results. With reference to the figure, the models predict the S_{11} and S_{21} reasonably well.

The lump microstrip coupled line filter is resonates at center frequency 2.14 GHz. The red colour electric field shows the strongest part that causes the center frequency.

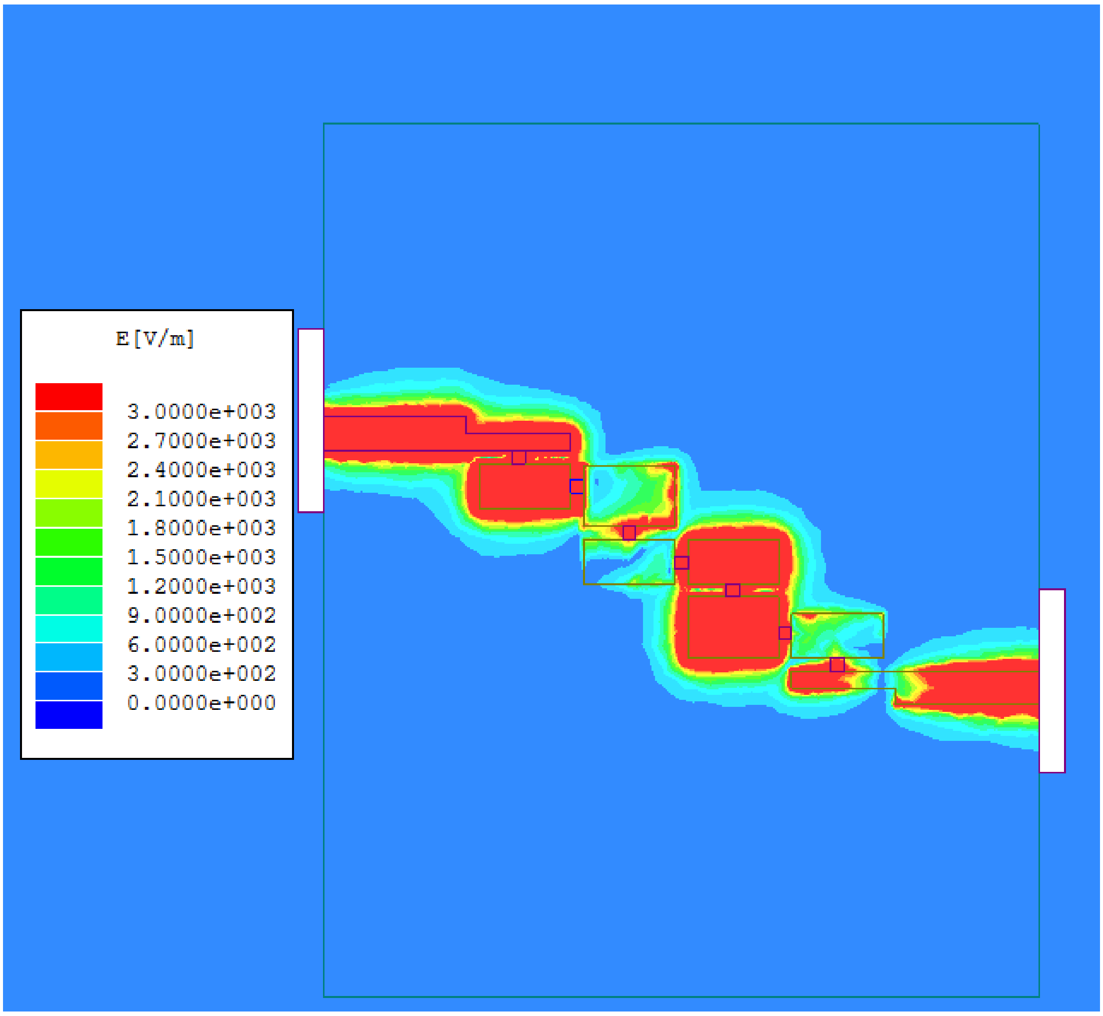

Figure 3.4: The electric field at 2.14GHz

The length of the lump coupled line filter is shorter than the original coupled line. Referring to the recent development in subtopic 2.2.2.1, the length of the 1.7GHz coupled line filter is 155mm, which is much longer than the current proposed lumped coupled line filter. This has proven the proposed filter designed using lump elements is working reasonably well and useful in size reduction.

3.1.4 Parameter Analysis

In this section, the parametric analysis is studied. The author needs to simulate the proposed filter using modified parameter with the same frequency range in order to ease the comparison. It aims to prove that values selected in configuration are able to perform better compare with other values. Different value of each design dimension was simulated and the results were discussed in this section.

The value of capacitor, C_1 used in this project is 3.3pF. By replacing C_1 value with 2.3pF and 4.3pF, the effects are illustrated in figure 3.5 below. It shows that capacitance of 3.3pF produced a wider band.

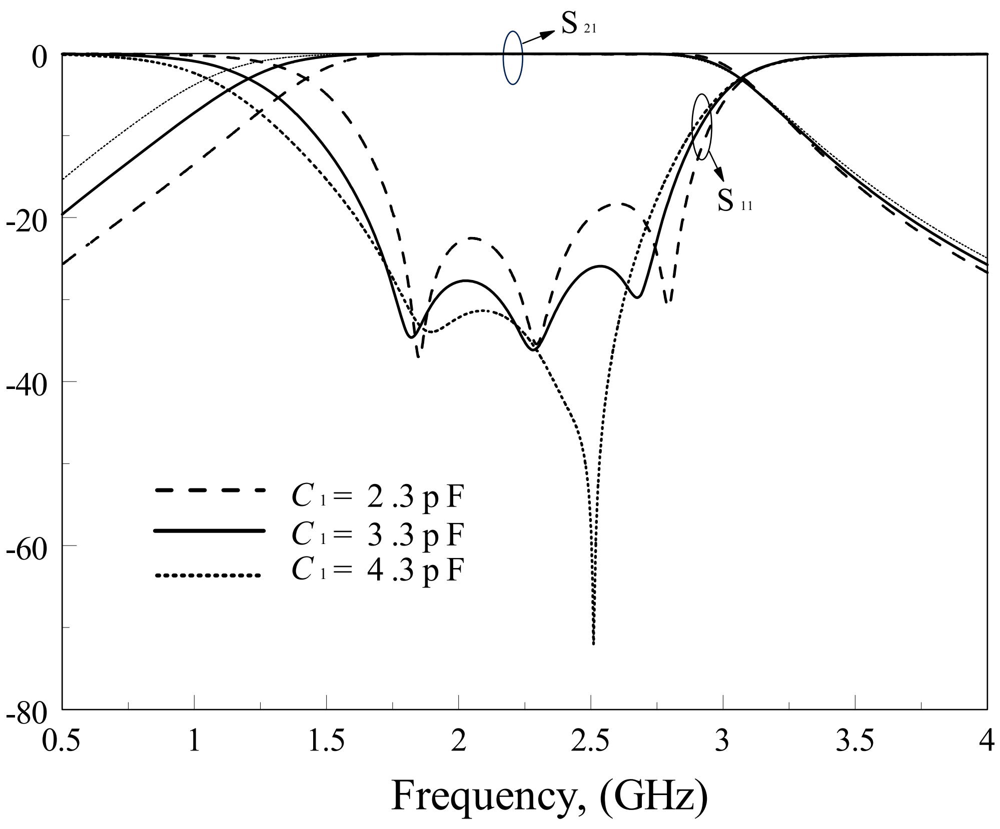

Figure 3.5: Effect of capacitance, C_1

The inductance of 2.2nH shows better matching result of the filter. For the inductance of 1.2nH and 3.2nH, the reflection loss is much higher and should be avoid in the pass-band. By observing the figure 3.6, the passband obviously is more influenced by the value of inductance. The value of inductors may not too large or too small to get the best impedance matching.

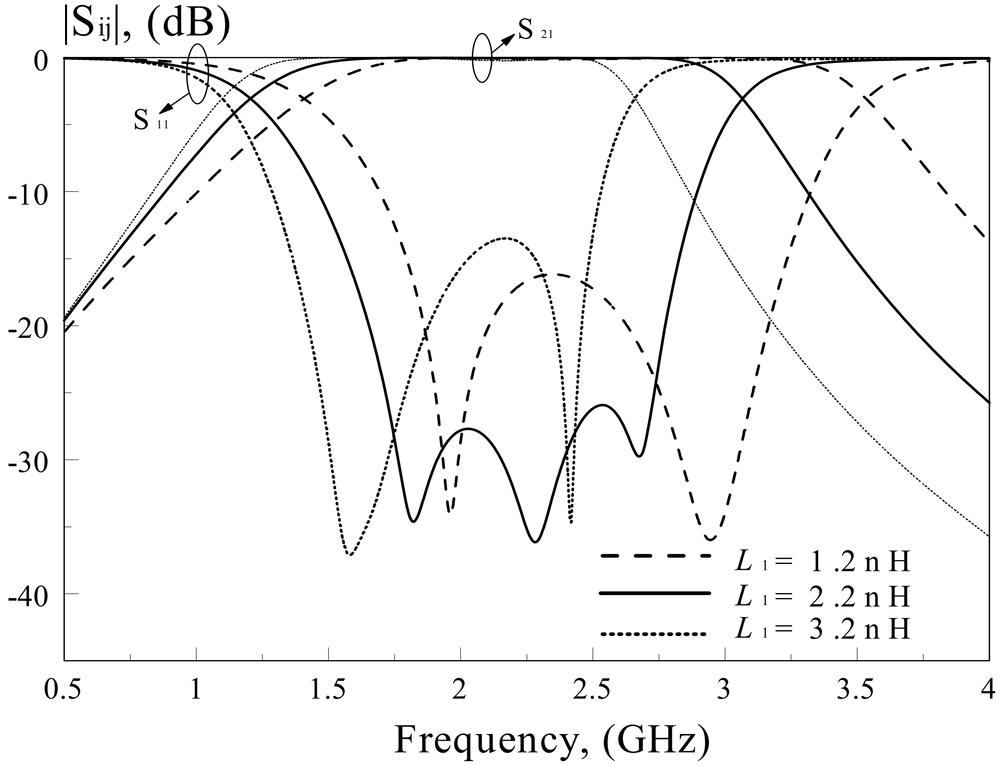

Figure 3.6: Effect of Inductance, L_1

3.2 LUMP MICROSTRIP COUPLED LINE FILTER (3 CAPACITORS)

3.2.1 Configuration

Here, multiple lump elements are implemented. Based on the previous filter configuration, each capacitor between two coupled lines is replaced with three capacitors. Figure 3.7 shows the proposed filter configuration.

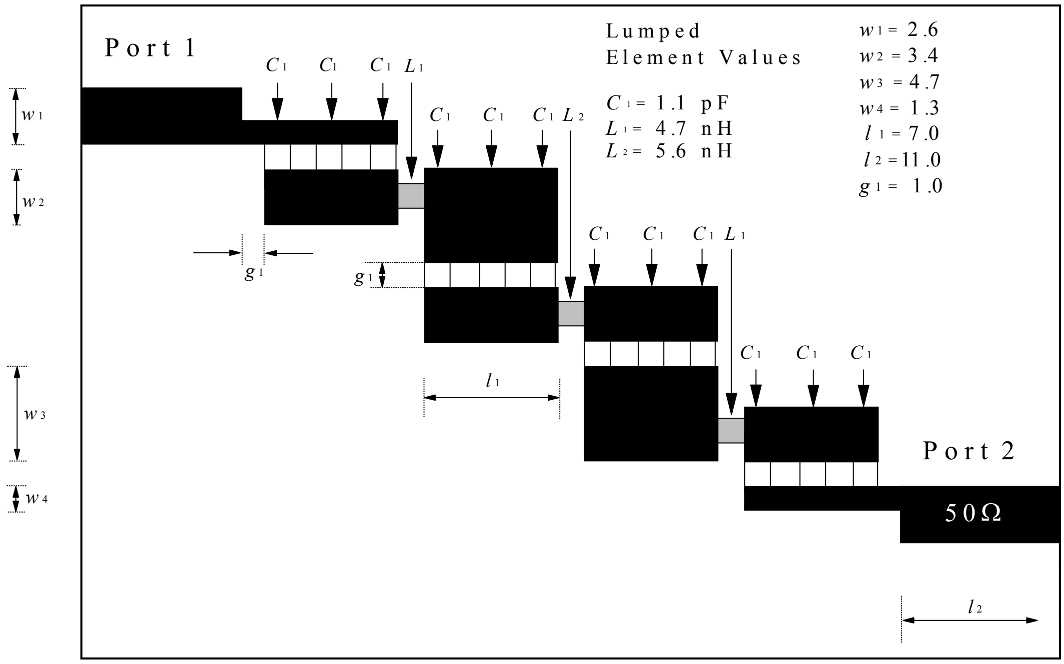

Figure 3.7: Top view of lump microstrip coupled line filter with 3 capacitors

Dimension of this lump microstrip coupled line filter is 67 x 55mm^2, same as figure 3.1. The filter parameters are l_1 =7 mm, l_2 =11 mm, g_2 =1 mm, w_1 =2.6 mm, w_2 =3.4 mm, w_3 =4.7 mm, w_4 =1.3 mm, similar with project 3.1. Three capacitors are arranged series in each of coupled line and the values were 1.1pF respectively. In the other hand, inductors values are increased for a good impedance matching, thus the second inductor, L_2 was introduced. The inductors values are stated clearly as figure 3.7 above which L_1 are equal to 4.7nH and L_2 is equal to 5.6nH.

3.2.2 Transmission Line Model

Equivalent circuit of proposed filter design is shown in figure 3.8. Modelling of 3 capacitors is more complex because have to divide into 8 parts for each block in this wiring revolution.

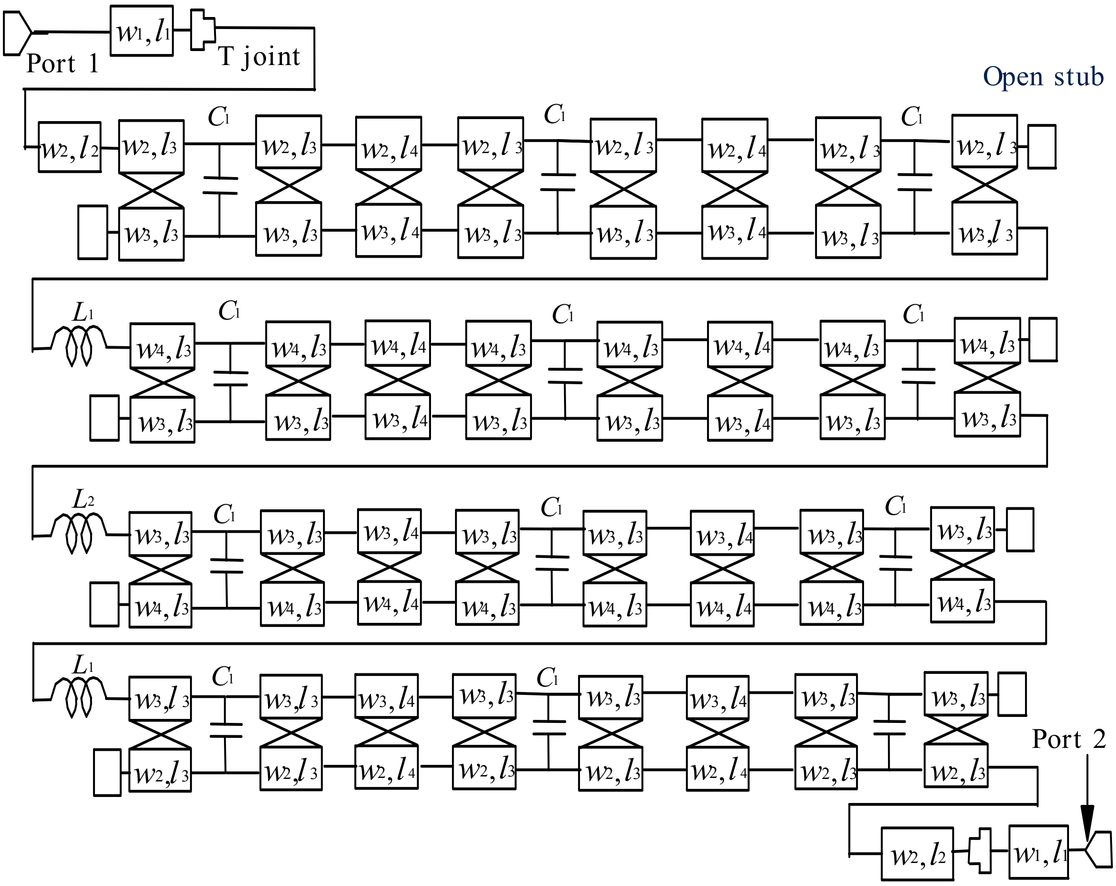

$w_1 = 2.6$
$w_2 = 1.3$
$w_3 = 3.4$
$w_4 = 4.7$
$l_1 = 11.0$
$l_2 = 1.0$
$l_3 = 3.5$
Unit in mm

Lumped
Element Values

$C_1 = 1.1$ pF
$L_1 = 4.7$ nH
$L_2 = 5.6$ nH

Figure 3.8: Equivalent circuit of lump microstrip coupled line filter with 3 capacitors

3.2.3 Results and Discussion

The result of lump coupled line microstrip filter with 3 capacitors is shown in Figure 3.9. The filter is resonated from 1.07 GHz to 2.46 GHz. The center frequency, bandwidth and error between measured and simulated results were calculated using formulas table 3.1 above.

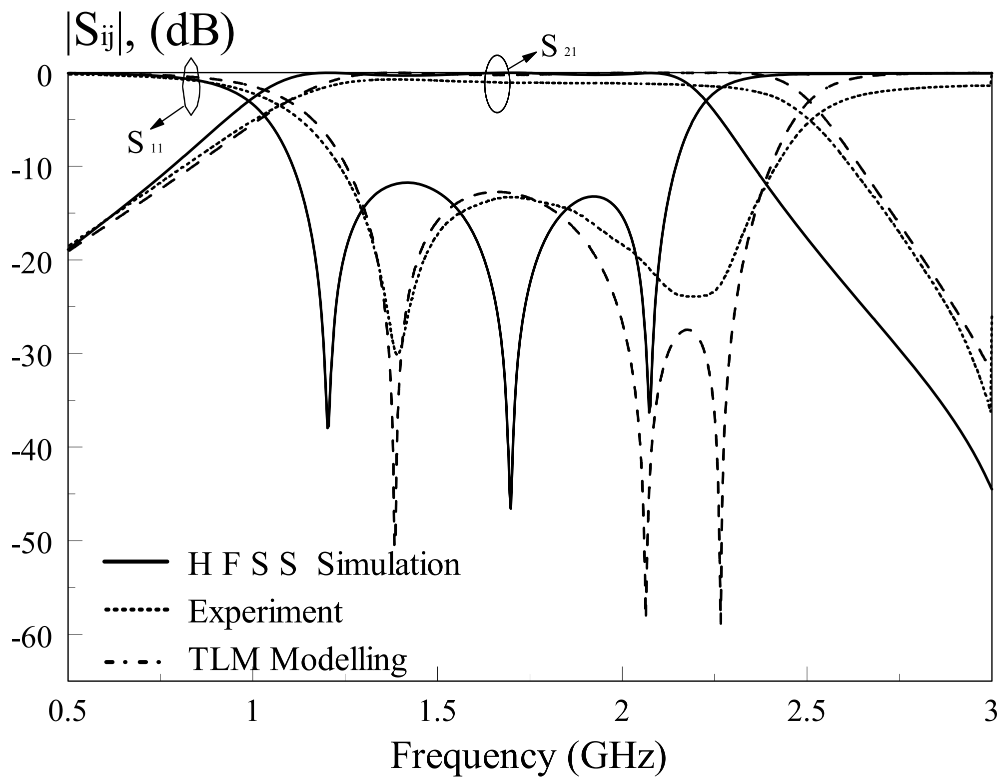

Figure 3.9: Measured and simulated S_{11} and S_{21} of lump microstrip coupled line filter with 3 capacitors

Figure 3.9 shows measurement and simulation results. The measured center frequency is 1.76 GHz, which is very close to the HFSS simulated value of 1.61 GHz (error 8.73%) and AWR simulated value of 1.80 GHz (error 2.22%). The measured and simulated 3-dB bandwidths ($|S_{11}| \leq -10$ dB) are given by 77.02%, 79.25% and 77.99% respectively. The results are summarized in table 3.3 for comparison.

Table 3.3: Comparison Results Table

	HFSS Simulated	Measured	AWR Simulated
Minimum Insertion Loss (dB)	-0.020	-0.721	-0.014
3-dB reference (dB)	-3.020	-3.721	-3.014
f_L (GHz) / f_H (GHz)	0.99/2.23	1.07/ 2.46	1.10/2.50
f_c (GHz)	1.61	1.76	1.80
Bandwidth (%)	77.02	79.25	77.99
Error (%)	8.73	-	2.22

Figure 3.10 shows the microstrip bandpass filter resonates at centre frequency 1.61 GHz. The red colour electric field shows the strongest part of the signal.

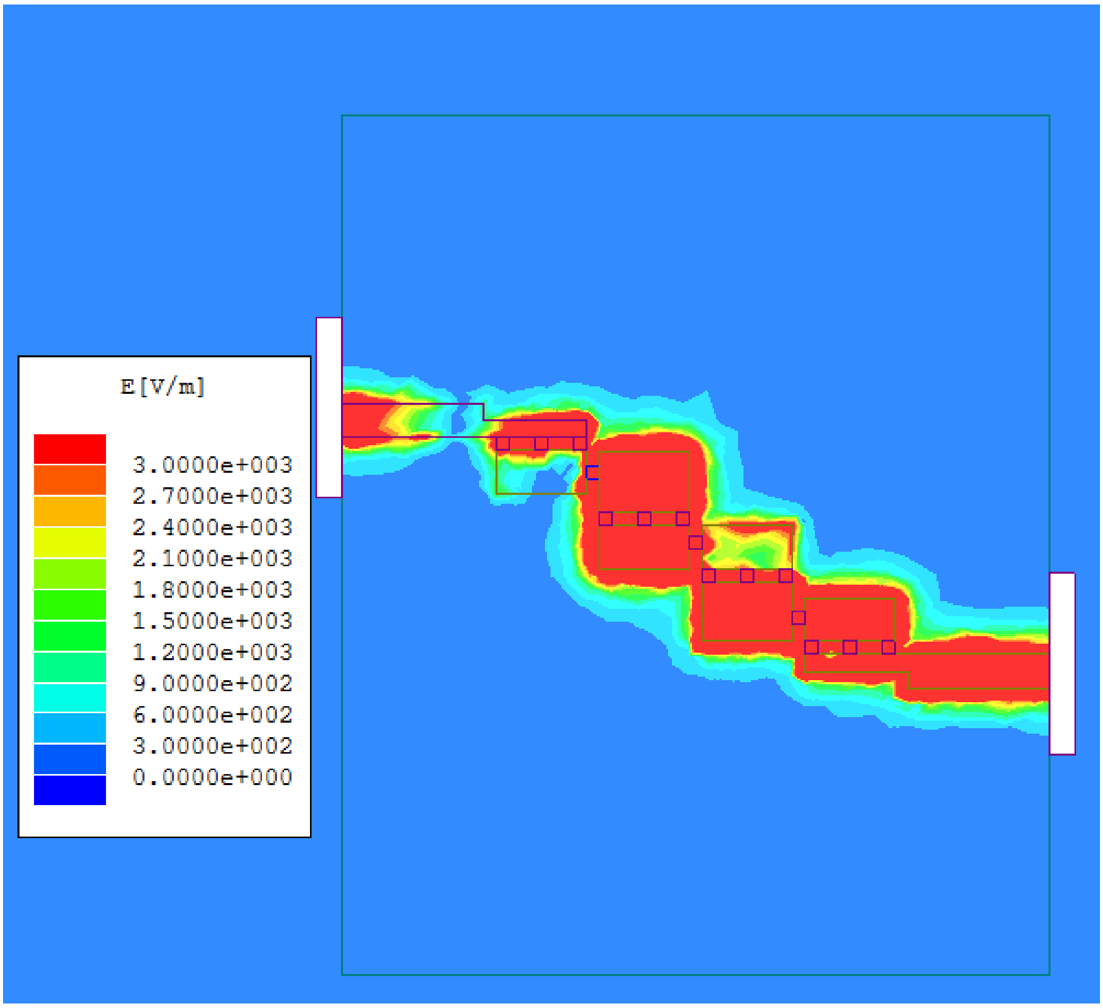

Figure 3.10: The electric field at 1.61GHz

3.2.4 Parameter Analysis

Capacitors values of 0.1pF, 1.1pF and 2.1pF are simulated. Effect of these three values can be view from figure 3.11.

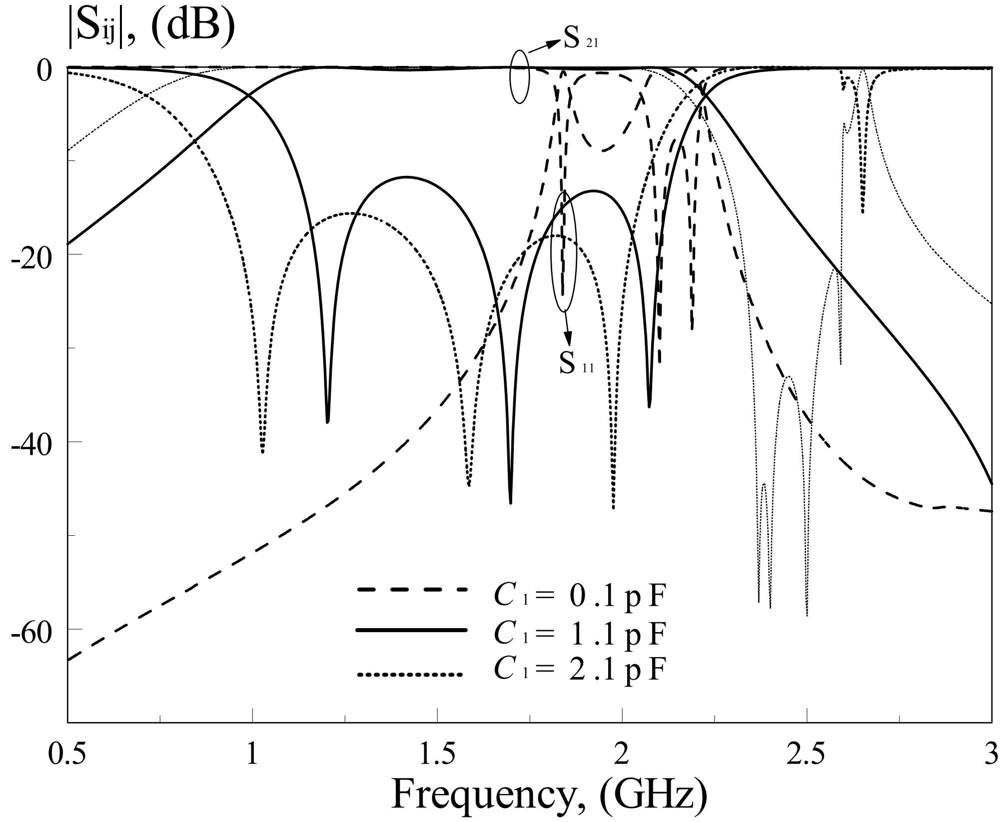

Figure 3.11: Effect of capacitance, C_1

Based on figure 3.11, capacitor value of 0.1pF was produced a lot of resonance frequencies, while capacitor value of 2.1pF was generated a distortion second harmonic wave. Hence, capacitor value of 1.1pF is obtained the best result. Two different value inductors were placed in the configuration to produce better filtering effect. Parameter analysis of inductors values are shown in figures 3.12 and 3.13.

First, capacitors, C_1 and middle inductor, L_2 were set as fixed variable, 1.1pF and 5.7nH respectively. The values L_1, 3.7nH, 4.7nH and 5.7nH were simulated Results are shown in figure 3.12.

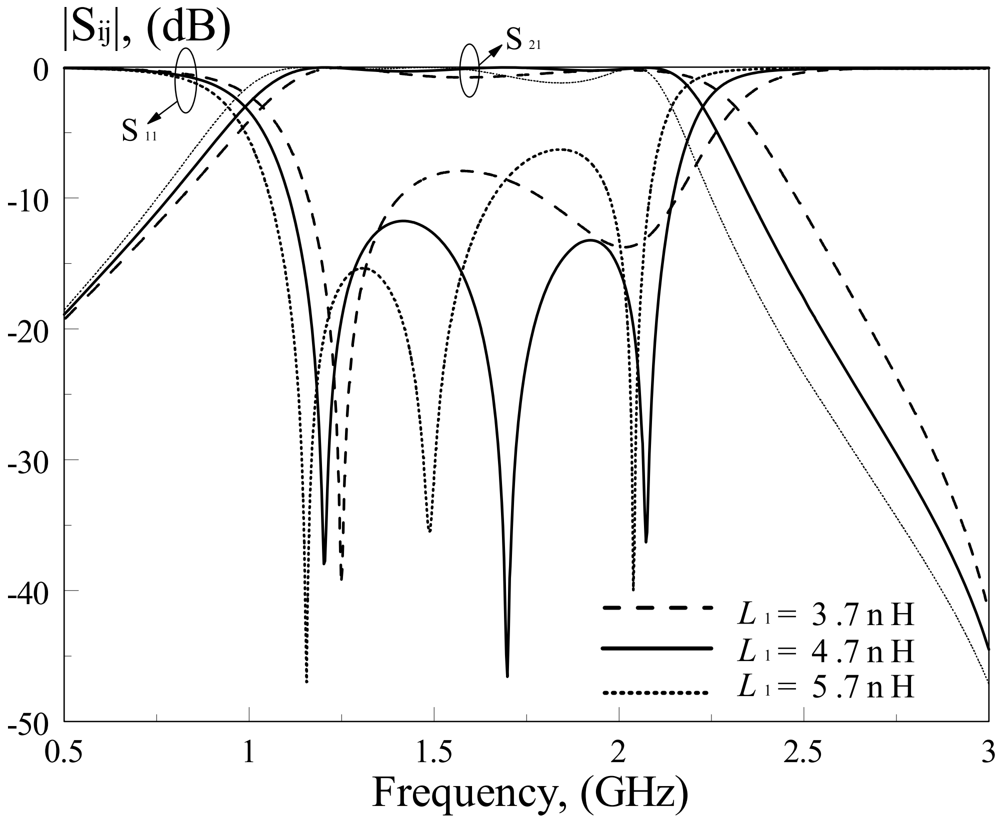

Figure 3.12: Effect of inductance, L_1

The inductors have tolerance value of ±0.5nH. When L_1 is 5.7nH, the value is approximately same with L_2, 5.6nH. It is inadequate while using the same inductance values through the entire microstrip line as higher insertion loss. Figure 3.12 shows the simulation of 3.7nH, 4.7nH and 5.7nH. Hence, 4.7nH is chosen for the proposed filter.

Figure 3.13 shows the effect of L_2 by varying 3 different values which are 4.7nH, 5.6nH and 6.8nH. Inductor, L_1 and capacitor, C_1 values were set as fixed variable. It shows again inadequate in the figure 3.13 when all inductors value is equal to 4.7nH. The reflection loss is higher when inductance value increases to 6.8nH. Hence, 5.6nH is the best choice for the middle inductor.

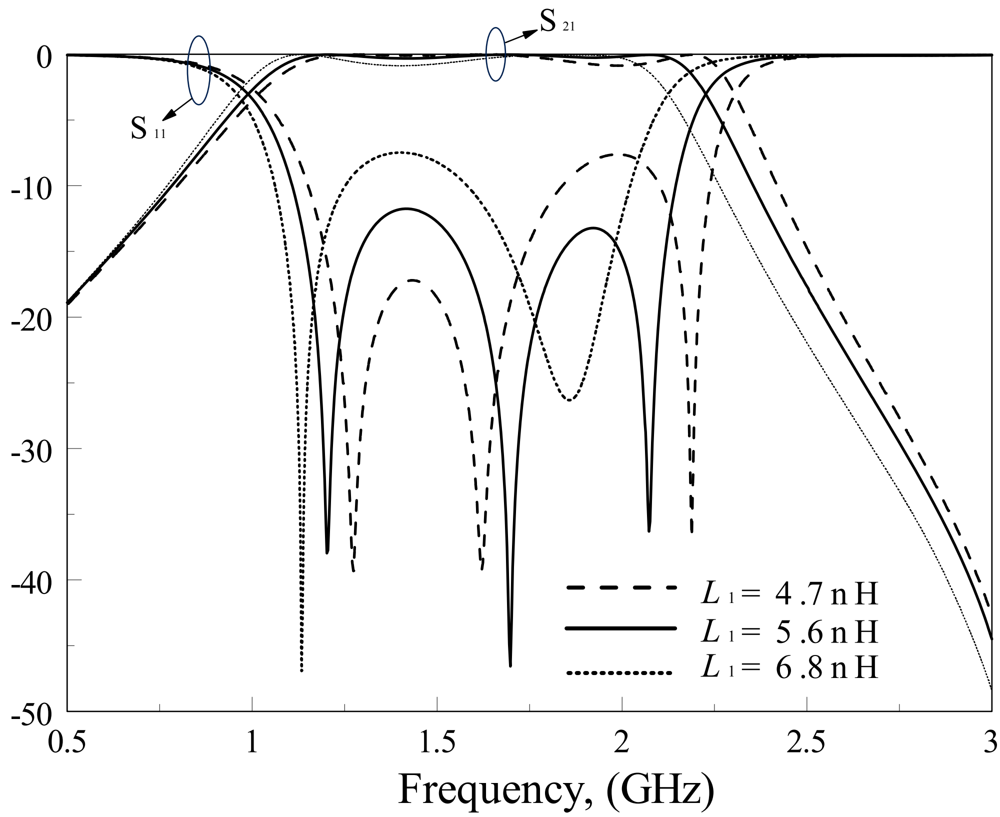

Figure 3.13: Effect of inductance, L_2

3.3 LUMP MICROSTRIP SQUARE RING FILTER

3.3.1 Configuration

In this subchapter, a lump microstrip square ring filter is proposed. Concept of this designed filter is to minimize the total size filter with only few inductors. FR_4 epoxy substrate was used in the designed filter, which relative permittivity, ε_r = 4.40 and thickness h = 1.57 mm.

The dimension of this proposed filter is 34.5 x 35mm^2. Parameters were stated in Figure 3.14 where l_1 =10 mm, p_1=5.15mm, p_2 =4.65mm, g_1 =0.2 mm, w_1 =6.0 mm, w_2 =0.5 mm, w_3 =3.0 mm, w_4 =0.3 mm and w_5 =2.7mm. Inductor value of L_1 is equal to 0.5nH.

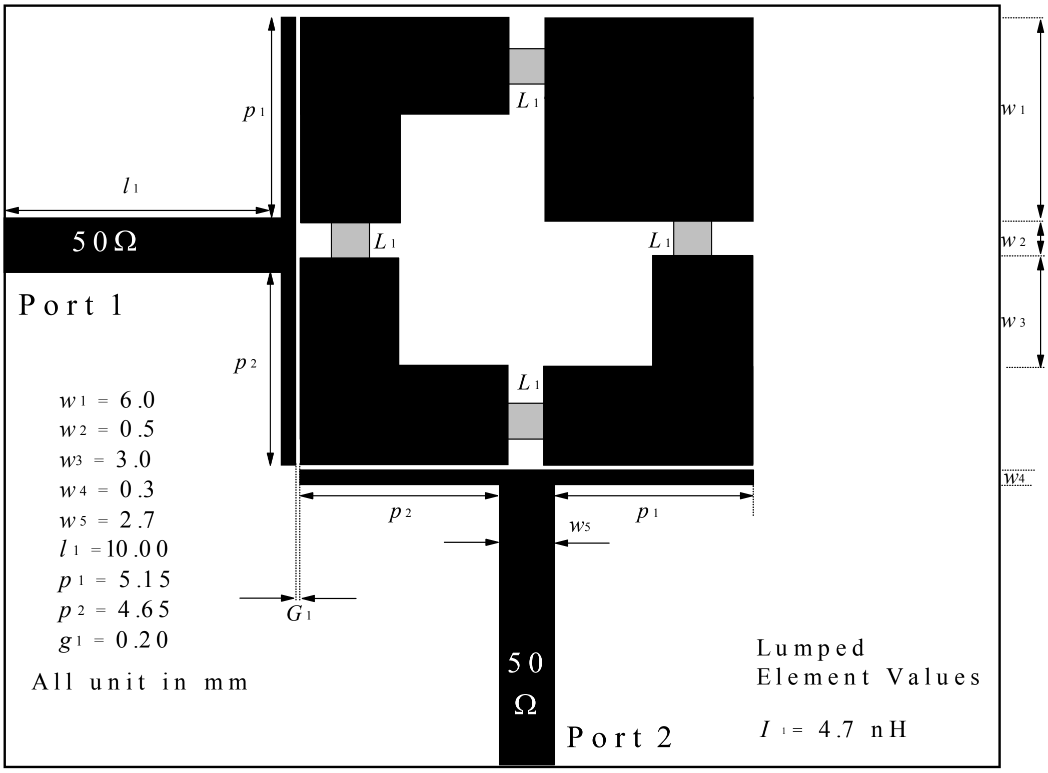

Figure 3.14: Top view of lump microstrip square ring filter

The gap distance, g_1 of this proposed filter is 0.2mm because 0.1mm gap is difficult to fabricate in the laboratory. It might be causing some error as the gap for capacitive coupling is extremely sensitive. Length of p_1 and p_2 were different to obtain better filtering effect. Width of the port, w_5 is set as 2.7mm in order to get 50ohm characteristic impedance. LQ0402, is the type inductor where placed between the two edges of coupled line. Thus it is small, so the width between two edges of coupled line,w_2 was set to 0.5mm for the placement inductor purpose.

3.3.2 Results and Discussion

The result of lump microstrip square ring filter is shown in Figure 3.15. From the figure, it can be observed that the proposed filter is designed successfully.

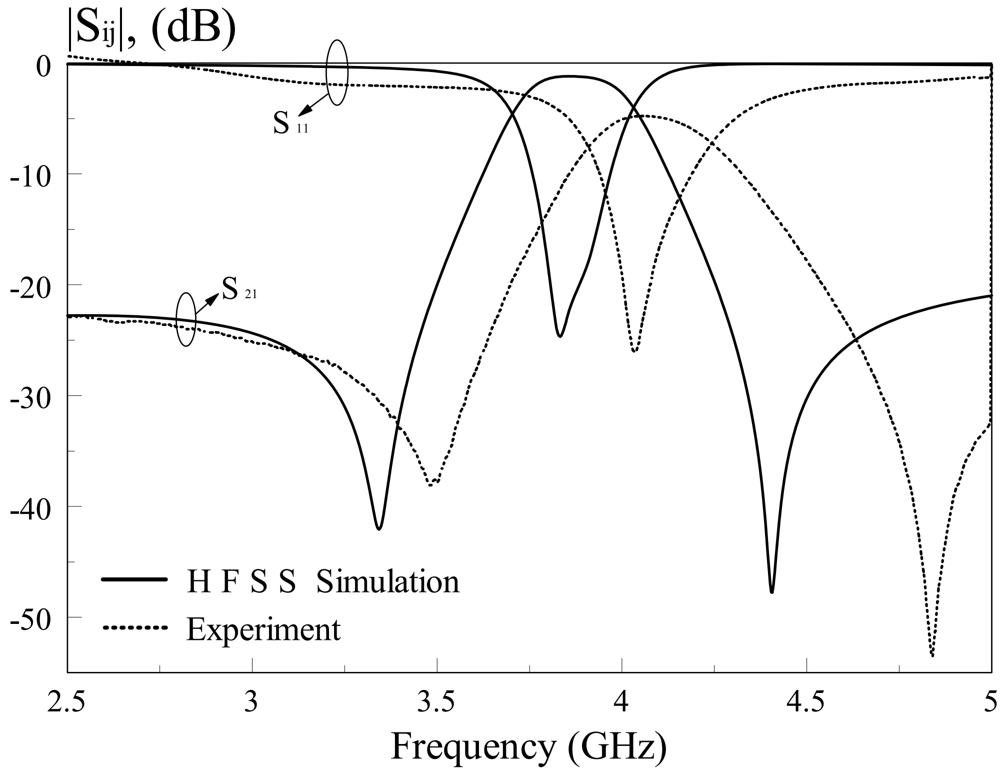

Figure 3.15: Measured and simulated S_{11} and S_{21} of lumped microstrip square ring filter

The measured proposed filter is resonates from 3.91 GHz to 4.60 GHz. From the measurement result, it shows that there are two transmission zeros in the passband which are 3.48 GHz and 4.84 GHz. The transmission zeros are used to improve the filter selectivity and the stopband rejection at the desired frequency. Referring to table 3.15, the center frequency (f_c), bandwidth and error between measured and simulated results were calculated.

The bandwidth normally decreases, at the faster rate, than the rate of element size reduction. Thus, in this case, the bandwidth percentage didn't decreases due to size reduction while compare with original square ring. Comparison of bandwidth calculation shows in table 3.4, results HFSS simulation between lump square ring and original square ring. The percentage of the bandwidth shows the lump square ring is working. Meanwhile, table 3.5 shows the performance results of lump square ring.

Table 3.4: Comparison percentage bandwidth between original and lump square ring

	HFSS	Simulated
	Original Square Ring	Lump Square Ring
Bandwidth (%)	7.94	8.27

Table 3.5: Comparison Results Table

	HFSS Simulated	Measured
Minimum Insertion Loss (dB)	-4.760	-1.183
3-dB reference (dB)	-7.760	-4.183
f_L (GHz) / f_H (GHz)	3.91/4.26	3.73/4.03
f_c (GHz)	4.08	3.87
Bandwidth (%)	16.99	8.27
Error (%)	5.42	-

The measured center frequency is 3.87GHz, very close to the simulated one, 4.08 GHz (error 5.42 %).This table shows excellent agreement between the simulated and measured data. Electric field is shown in the figure 3.16. Red colour is indicated the strongest part that causes the center frequency of 4.08GHz.

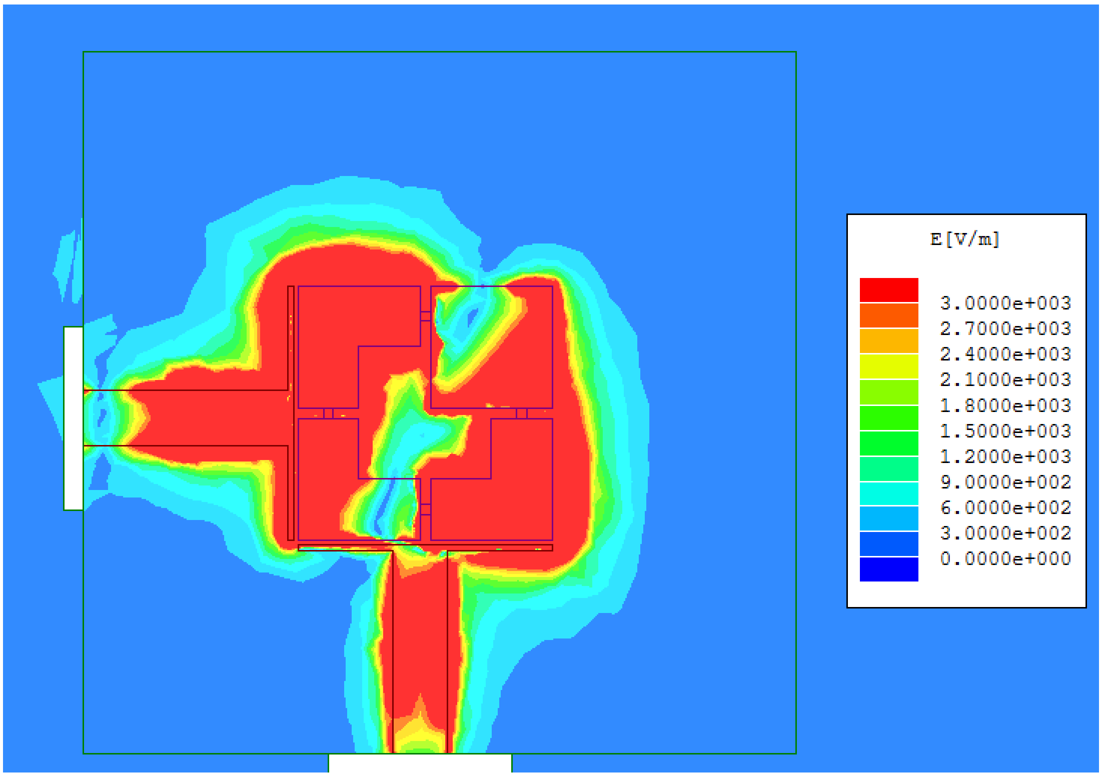

Figure 3.16: The electric field at 4.08GHz

3.3.3 Parameter Analysis

The novelty of the proposed filter is miniature size. In order to reduce the size filter, inductors were used as the replacement for the transmission line. So, the inductance value becomes the main issue in this analysis.

Figure 3.17 shows how the inductance values affect the filtering result. Three typical values of inductance, 0.1nH, 0.5nH and 1.5nH were simulated. The effects of these values were investigated. It is observed that, there is no influence on signal bandwidth but frequency shifted when the inductors values changed. Hence author chose 0.5nH for the proposed filter.

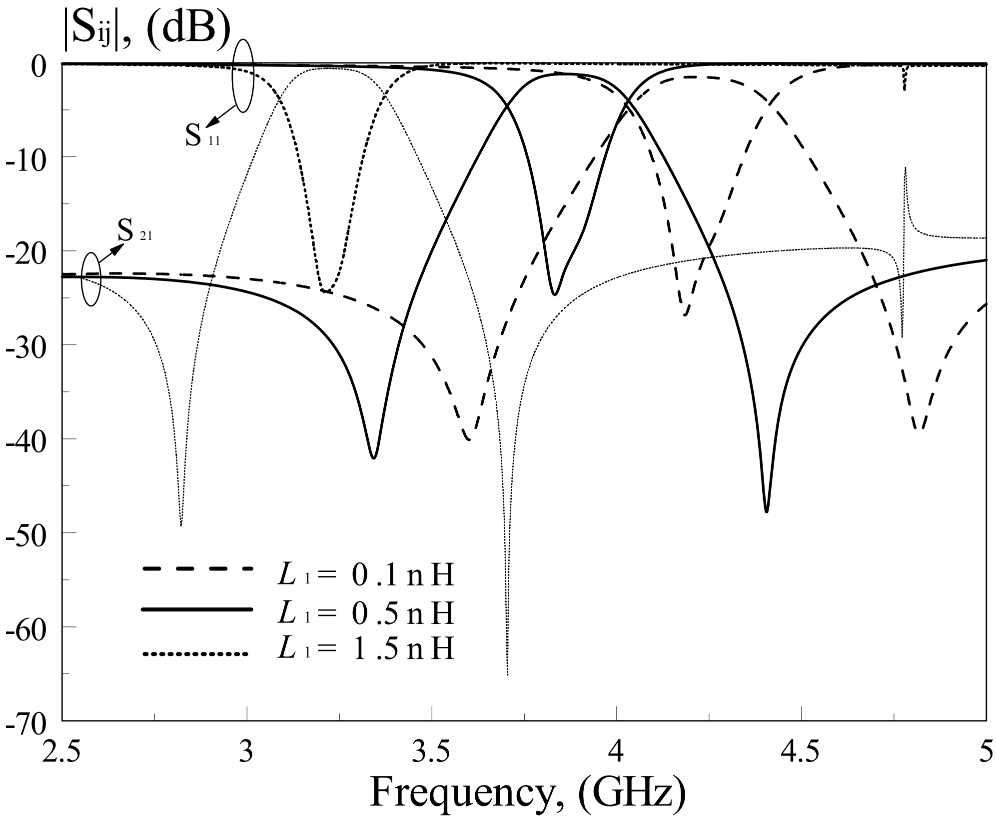

Figure 3.17: Effect of inductance, L_1

Width of the port, w_4 is adjusted between 3 parameters: 0.2mm, 0.3mm and 0.4mm.The result is shown in figure 3.18. It is observed that w_4 has no influence on the resonance frequency, but the input impedance is slightly decreases when signal bandwidth is increases. Adjust the parameter w_4 might be thoughtful instead to increases bandwidth signal of this filter. However, it is not the main issue in this research project.

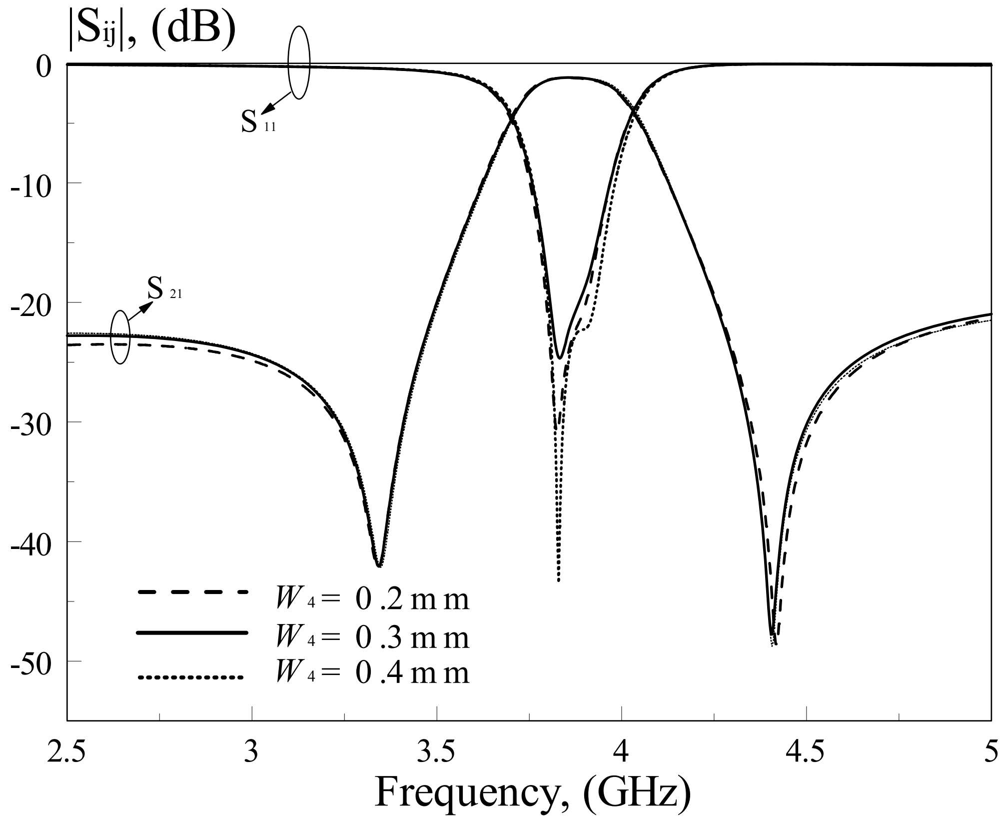

Figure 3.18: Effect of width, W_4

CHAPTER 4

POWER DIVIDER

4.1 LUMP MICROSTRIP COUPLED LINE POWER DIVIDER (1 CAPACITOR)

4.1.1 Configuration

In this chapter, the characteristics and design parameters of lump coupled line power dividers are discussed. The configuration of the lump coupled line power divider with 1 capacitor is shown in Figure 4.1.

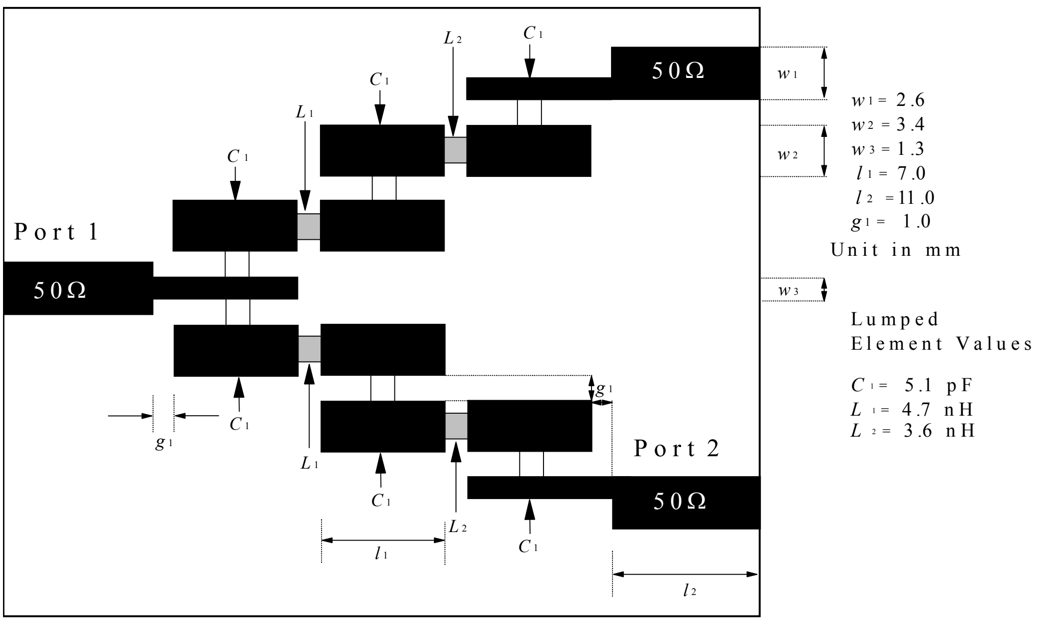

Figure 4.1: Top view of lump coupled line power divider with 1 capacitor

A FR_4 epoxy substrate with relative permittivity, ε_r = 4.40 and thickness h = 1.57 mm was used in this proposed power divider. The dimension of the power divider is 60 x 47mm^2. Parameters were described as l_1 =7 mm, l_2 =11 mm, g_1 =1 mm, w_1 =2.6 mm, w_2 =3.4 mm, w_3 =1.3 mm. Capacitor, C_1 is defined as 5.1pF. Inductors values of L_1, L_2 is equal to 4.7nH and 3.6nH respectively.

4.1.2 Transmission Line Model

Equivalent circuit of transmission line model is shown in figure 4.2. Each block divided into 2 parts which length of 3.5mm. Parameters are described clearly in figure as well.

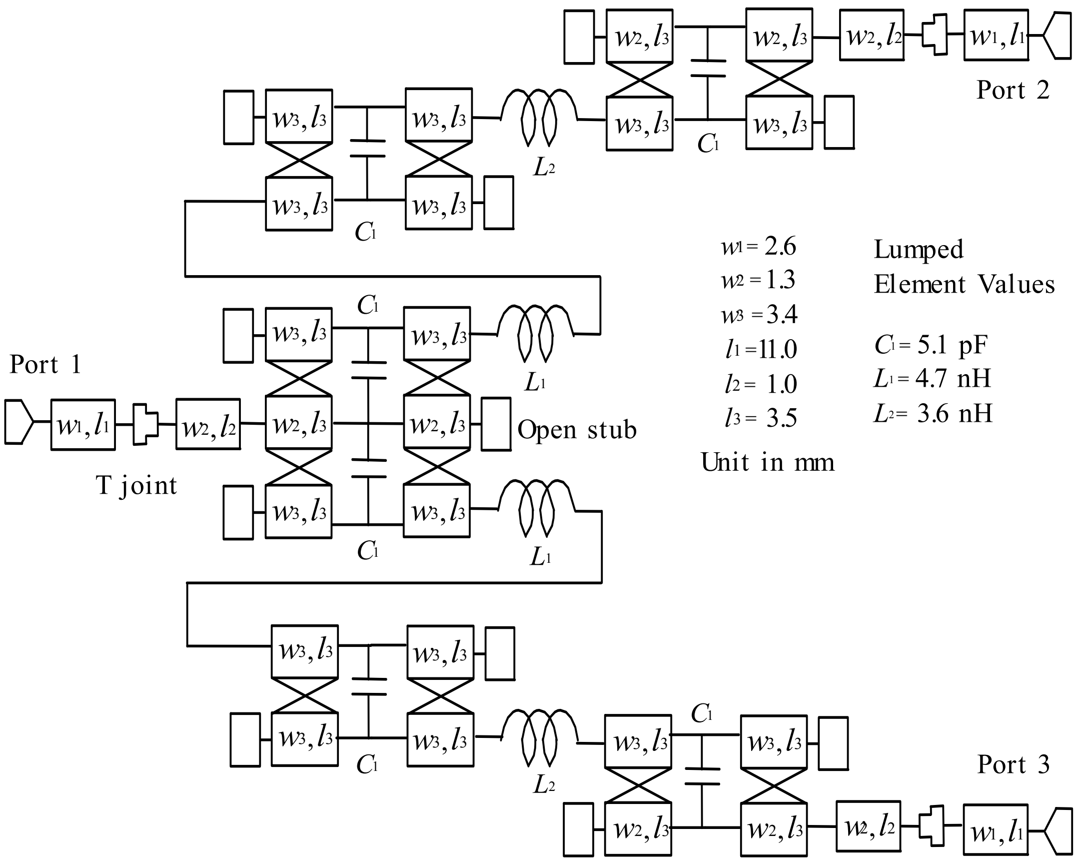

Figure 4.2: Equivalent circuit of lump microstrip coupled line power divider with 1 capacitor

4.1.3 Results and Discussion

All the measurements are done by using Rohde & Schwarz Vector Network Analyzer ZVB8 (VNA). The result of the lumped coupled line microstrip power divider with 1 capacitor is shown in Figure 4.3.

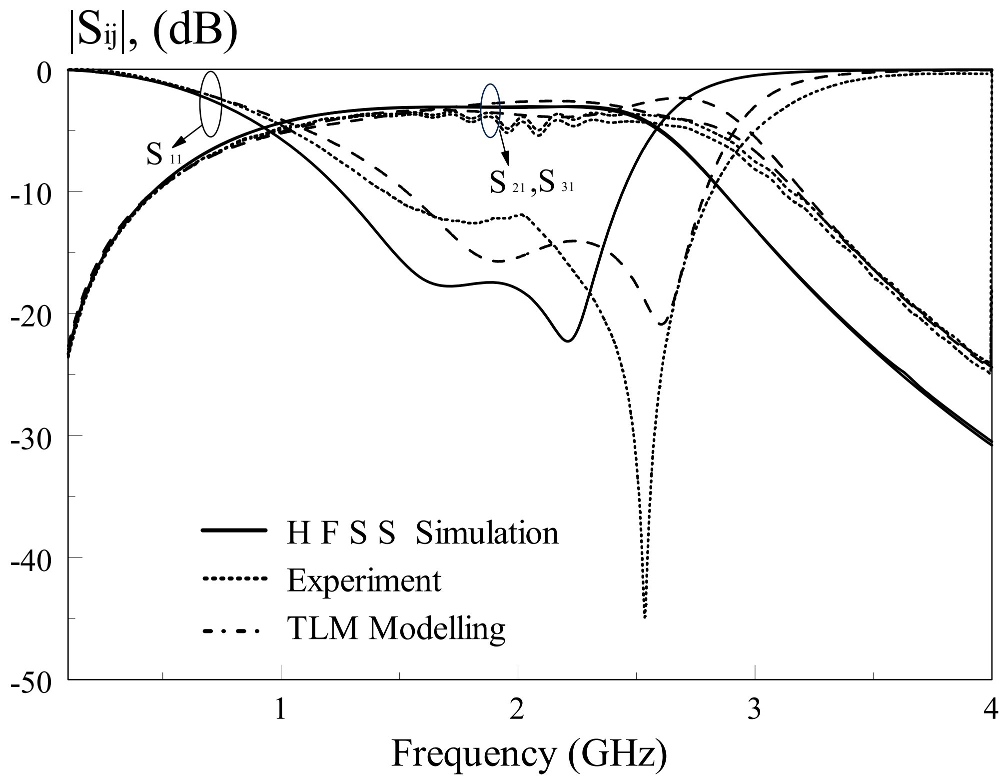

Figure 4.3: Measured and simulated S_{11}, S_{21} and S_{31} of lumped microstrip coupled line power divider with 1 capacitor

Figure 4.10 shows the simulated and measured S-parameters of the proposed power divider and both of them agreed very well. The center frequency, fractional bandwidth and error between measured and simulated result were calculated by using the formulas given in previous chapter. The data was summarized in table 4.1 for comparison.

Table 4.1 Comparison Results Table

	HFSS Simulated		Measured		AWR Simulated	
	S_{21}	S_{31}	S_{21}	S_{31}	S_{21}	S_{31}
Minimum Insertion Loss (dB)	-3.044	-3.039	-3.450	-3.690	-2.590	-2.350
3-dB Reference (dB)	-6.044	-6.039	-6.450	-6.690	-5.290	-5.350
f_L (GHz) / f_H (GHz)	0.77 /2.66	0.76 /2.67	0.77 / 2.93	0.74 /2.91	0.92 /2.92	0.96 /2.99
f_c(GHz)	1.72	1.72	1.85	1.83	1.92	1.98
Bandwidth (%)	109.88	110.04	116.76	118.58	104.17	102.52
Error (%)	7.56	6.40	-	-	3.78	8.20

From the table 4.1, it shows the bandwidth percentage of the proposed design is high where within the range of ultra-wide band. The error percentages of HFSS simulated and AWR simulated are consider low (within 10% difference). Thus measured result verified well with simulated results.

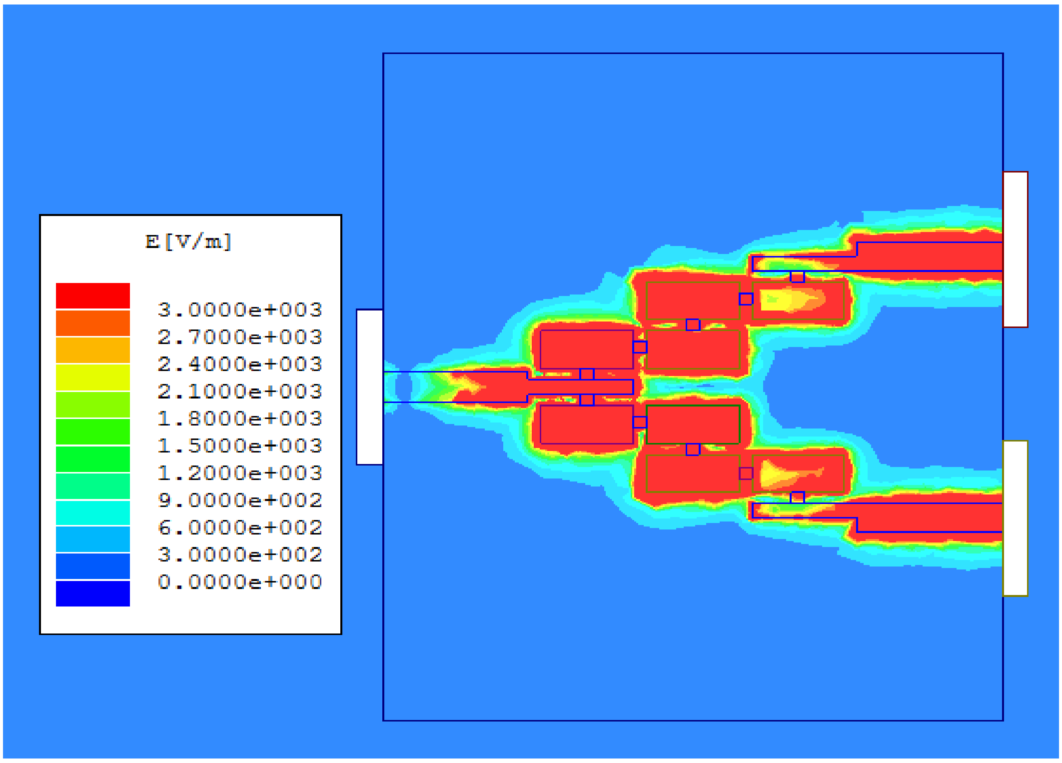

Figure 4.4: The electric field at 1.72GHz

Figure 4.4 shows the electric field where resonates at 1.72GHz .The red colour shows the strongest part of the electric field.

4.1.4 Parameter Analysis

Each of the power divider parameter that affects the result will be manipulate during the case study. It aims to study the effect on modified parameters and find out any of it that will improve the power divider performance. For example lower power consumption, wider passband, simpler configuration, and others. In this case study, the parameter analysis will mainly focus on the values of lump elements.

Different value of lump elements is studied accordingly .The analysis of lump element values can be divided into capacitance and inductance. The parametric analysis is firstly performed with capacitance C_1 , where result shown in figure 4.5.

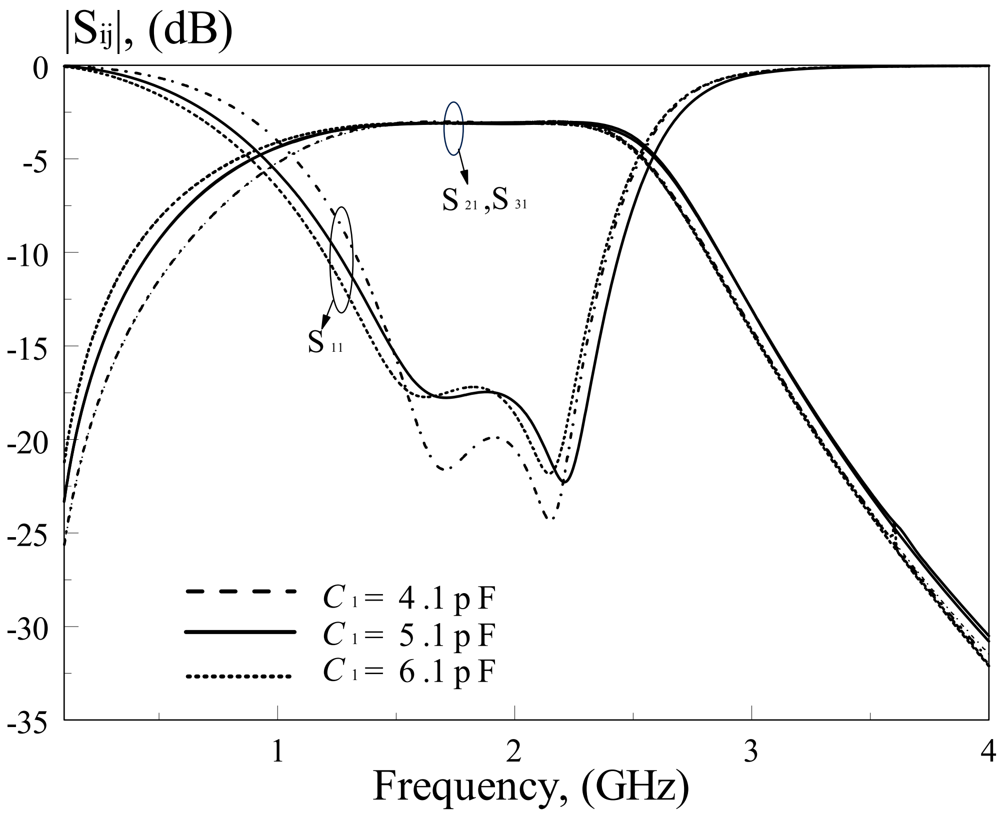

Figure 4.5: Effect of capacitance, C_1

It observed that passband does not deteriorated much while varying the value C_1. This indicated that capacitance value is not the main factor in the proposed design. Hence, author had chose 5.1pF for the value C_1,.

In the following parameter analysis, author has fixed the value of capacitance C_1 and inductance value L_2. The manipulation of parameter value is performed on inductors L_1, which measured value is 4.7nH in proposed filter configuration.

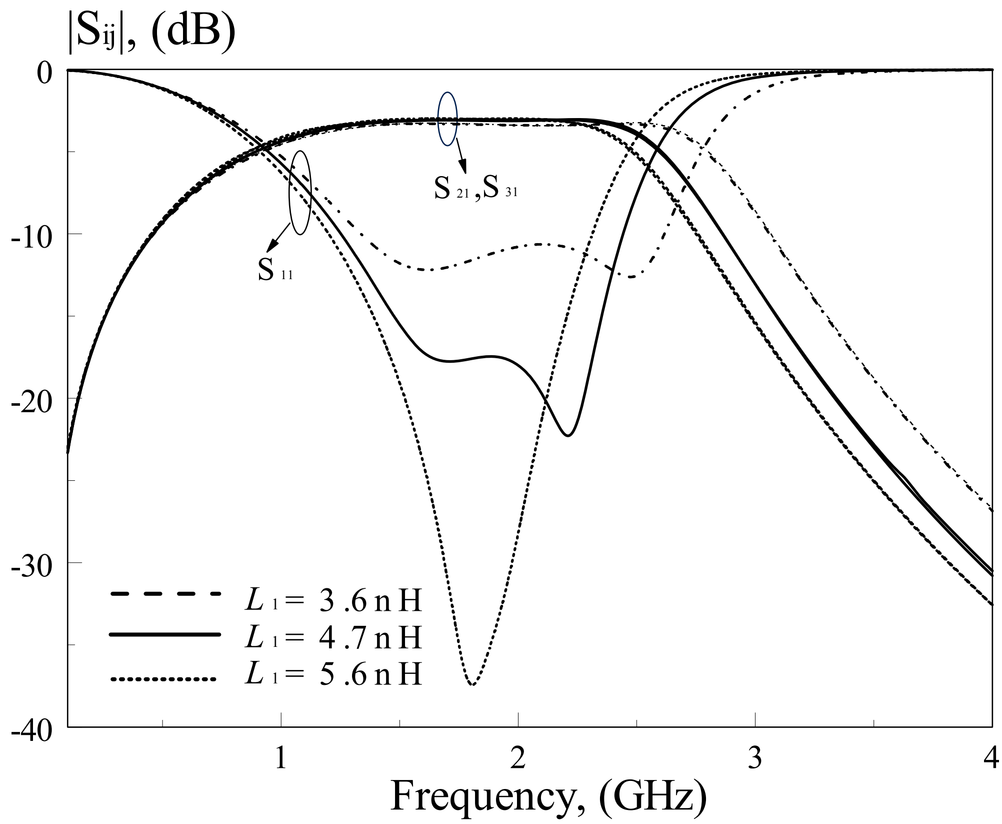

Figure 4.6: Effect of inductance, L_1

Next, author has simulated the configuration again by varying the value of L_2. The initial selected value for L_2 is 3.6nH where located at the second section of the lump coupled line power divider. Three typical values of inductance, 2.2nH, 3.6nH and 4.7nH were simulated.

Referring to the figure 4.7, the return loss (S_{11}) in the passband decayed further again to -20 dB and yet the blending of the two poles is diminished when the inductance value is 2.2nH. Then author has increased the value L_2 to 4.7nH, which same value as L_1. Thus, the return loss, S_{11} is raised closer to -10dB due to poor matching and again has proven the same inductance values in this power divider will reduce the performance for the signal transmission.

As a result, same value in all inductors has a big impact on the return loss within the passband. Value L_2 is preferred less than L_1 to achieve better impedance matching.

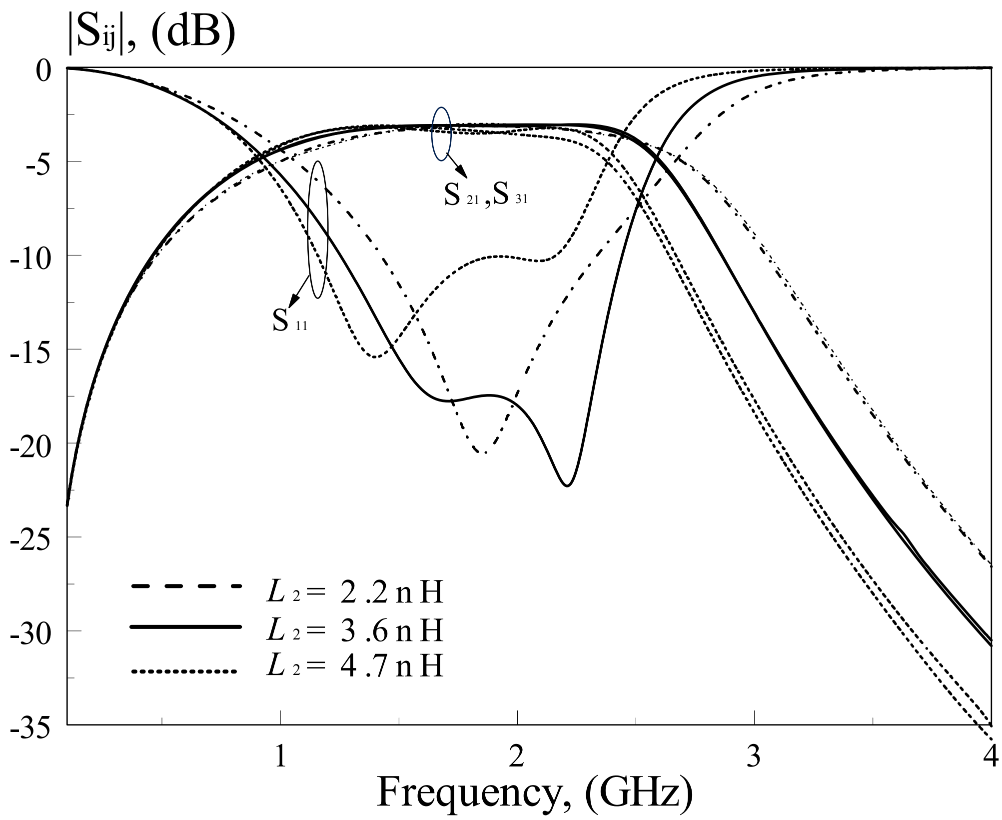

Figure 4.7: Effect of inductance, L_2

4.2 LUMP MICROSTRIP COUPLED LINE POWER DIVIDER (3 CAPACITORS)

4.2.1 Configuration

Another lump coupled line power divider is proposed but configuration is same as subtopic 4.1. Thus, three capacitors were located between all the coupled lines accordingly. Configuration of the proposed filter is shown in Figure 4.2.

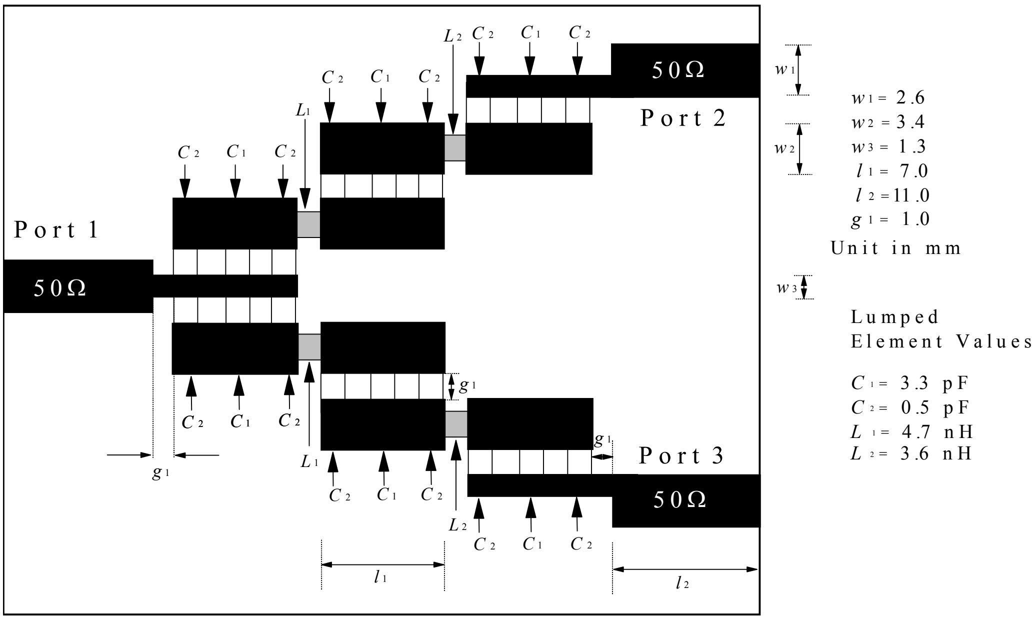

Figure 4.8: Top view of lump coupled line power divider with 3 capacitors

A FR_4 epoxy substrate with relative permittivity, ε_r = 4.40 and thickness, h = 1.57 mm was used in this proposed design. The dimension of the power divider is 60 x 47mm^2. Parameters are described as: l_1 =7 mm, l_2 =11 mm, g_1 =1 mm, w_1 =2.6 mm, w_2 =3.4 mm, w_3 =1.3 mm. Capacitors, C_1 and C_2 are 3.3pF and 0.5pF, while inductors, L_1 and L_2 are 4.7nH and 3.6nH respectively.

4.2.2 Transmission Line Model

Details of equivalent circuit structure are described in figure 4.9.Each of the coupled lines is presented by wiring structure, M2CLIN and M3CLIN in the AWR software. The equivalent circuit is more complex as it has to consider all the subsections of a transmission line.

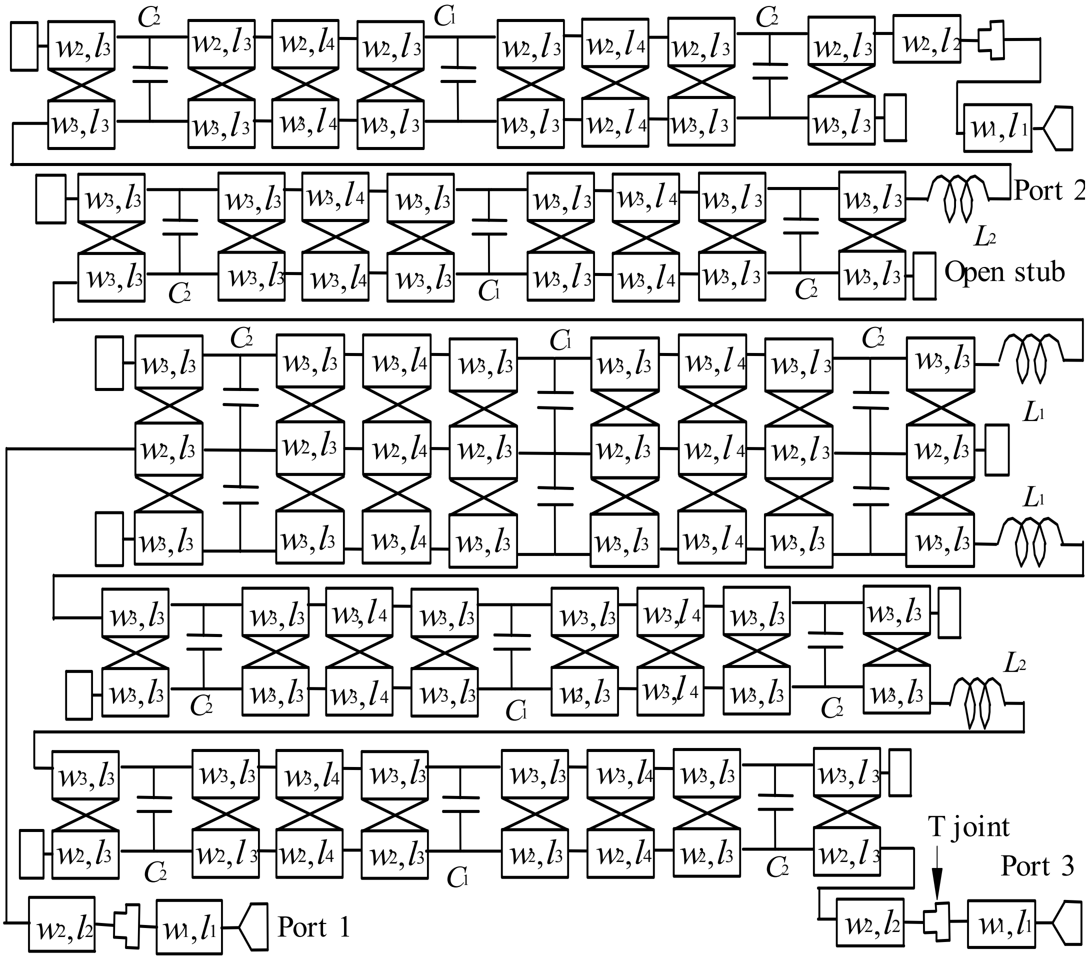

w_1 = 2.6
w_2 = 1.3
w_3 = 3.4
l_1 = 11.0
l_2 = 1.0
l_3 = 0.5
l_4 = 2.0
Unit in mm

Lumped Element Values

C_1 = 0.5 pF
C_2 = 3.3 pF
L_1 = 4.7 nH
L_2 = 3.6 nH

Figure 4.9: Equivalent circuit of lump microstrip coupled line power divider with 1 capacitor

4.2.3 Results and Discussion

Figure 4.10 shows the comparison results between measured result and simulated results of the proposed power divider. The return losses or S-parameters (S_{11}, S_{21} and S_{31}) are described in the plotted graph and results are verified well. Thus, the desired microstrip power divider is designed successfully.

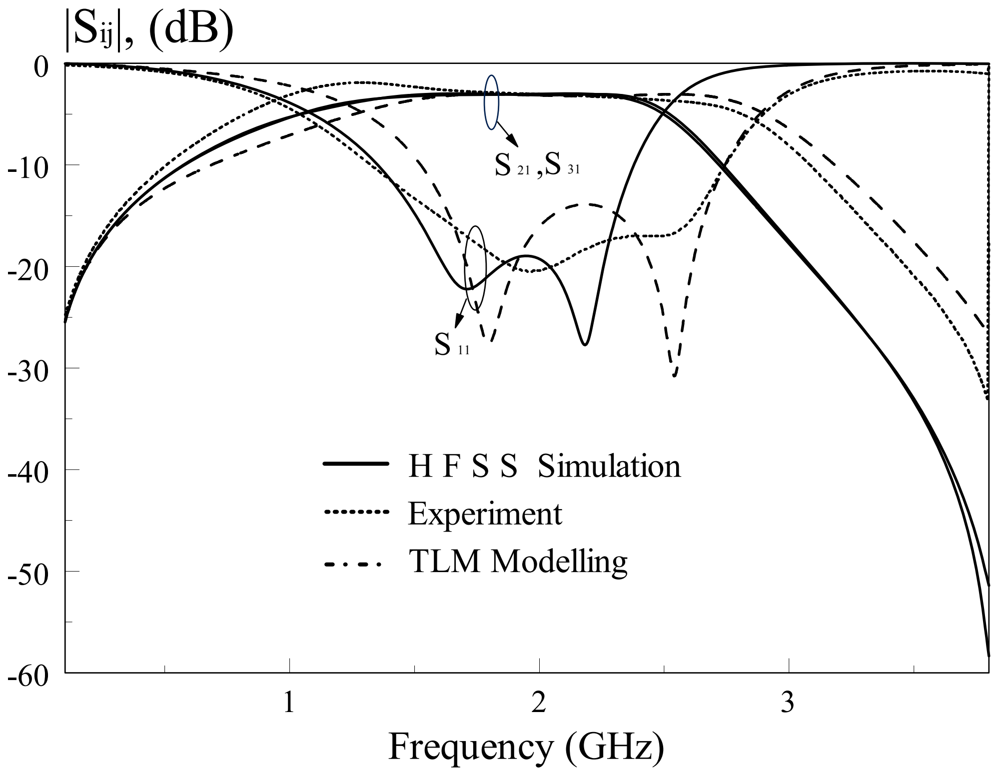

Figure 4.10: Measured and simulated S_{11}, S_{21} and S_{31} of lumped microstrip couple line power divider with 3 capacitors

Referring formulas in Table 3.1, calculation which included center frequency, bandwidth and error between measured and simulated results are shown in table 4.2. From the table, the percentages error between the simulation results and the experimental results are slightly more than 10%. The discrepancy in simulation results is mainly due to the increasing of capacitors in the structure. Due to the effect of lump elements, the design is being pushed to the limit to obtain the good result.

Table 4.2 Comparison Results Table

	HFSS Simulated		Measured		AWR Simulated	
	S_{21}	S_{31}	S_{21}	S_{31}	S_{21}	S_{31}
Minimum Insertion Loss (dB)	-2.981	-2.982	-1.900	-1.900	-3.045	-3.045
3-dB Reference (dB)	-5.981	-5.982	-4.900	-4.900	-6.045	-6.045
f_L (GHz) / f_H (GHz)	0.91 /2.58	0.93 /2.55	0.83 /2.80	0.83 /2.80	1.13 /2.97	1.13 /2.97
f_c(GHz)	1.75	1.74	1.82	1.82	2.05	2.05
Bandwidth (%)	95.70	93.10	108.54	108.54	90.19	90.19
Error (%)	11.83	14.23	-	-	16.91	16.91

However, the bandwidth percentage is high which may considered as wide band. Meanwhile electric field can be observed in figure 4.11 during the resonant frequency and shows the signal is able to transfer through the power divider.

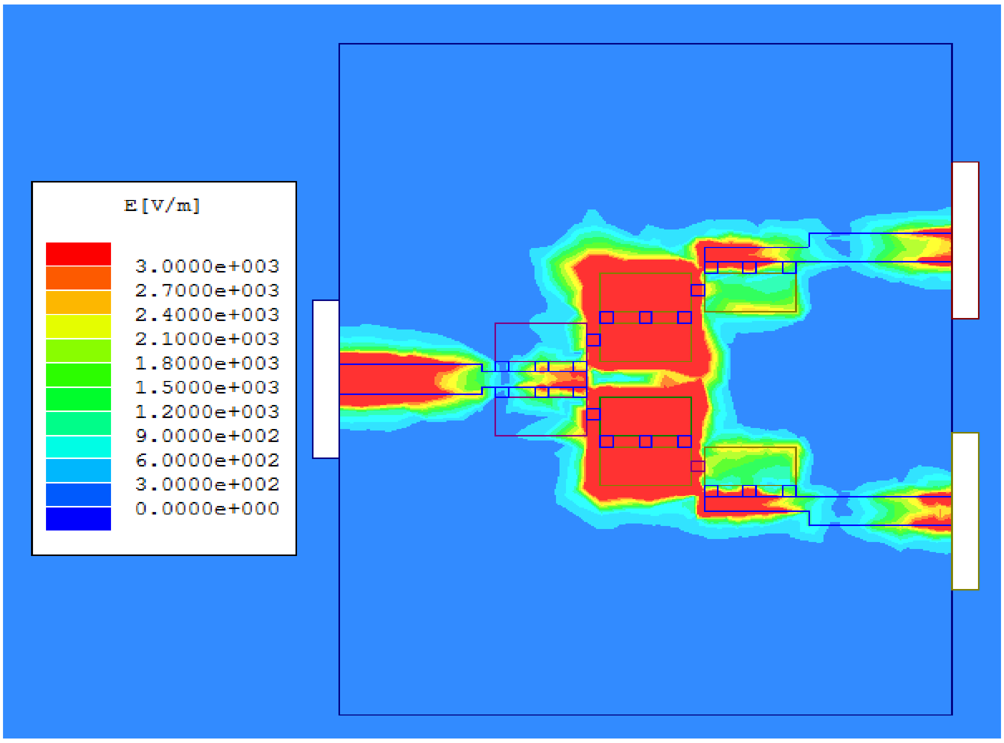

Figure 4.11: The electric field at 1.75GHz

4.2.4 Parameter Analysis

In this case study, the behaviour of each lump element in the power divider has been analyzed. It aims to find out any modification value of the parameter that will improve the power divider performance. The analysis shows all the parameters have been optimized. Frequencies were set as constant variables for better comparison. Firstly the parameter get started with value of capacitor, C_1 where located in the every middle slot of the coupled lines. Result is shown in figure 4.12.

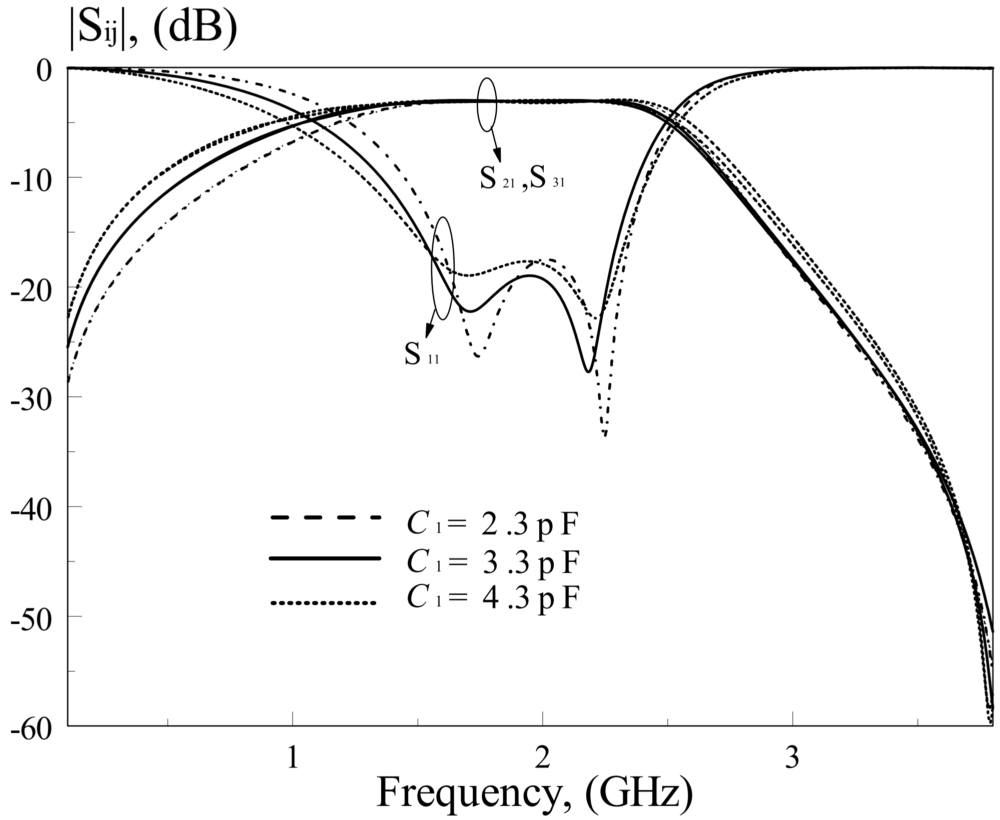

Figure 4.12: Effect of capacitance, C_1

There is no significant effect as the value of capacitor, C_1 increased from 2.3pF to 4.3pf. Hence 3.3pF is chosen to ease the soldering progress. The author re-simulates the configuration with varying the capacitor value C_2 while the capacitor, C_1 is set as fixed variable. C_2 is prefers to be smaller value where simulated using 0.1pF, 0.5pF and 1pF typically. It can be observed that capacitors values did not affect much on the entire passband performance.

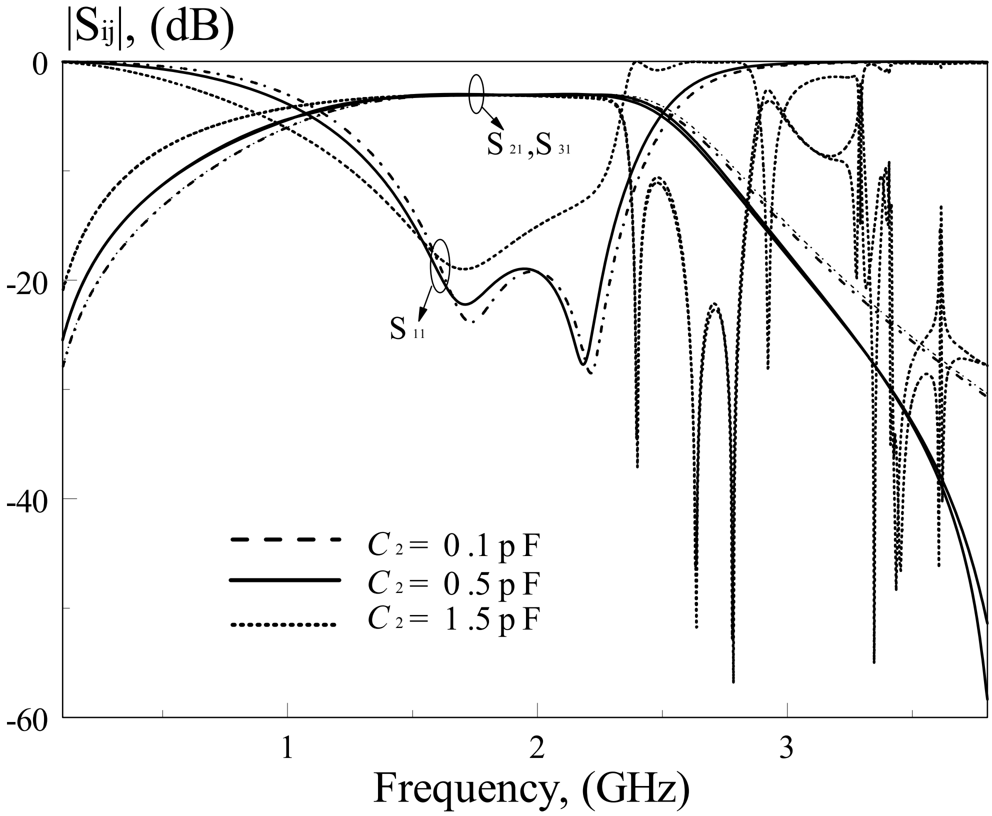

Figure 4.13: Effect of capacitance, C_2

Referring to the figure 4.13, effect C_2 to the passband is not obvious when it is 0.1pF. By applying capacitor value of 1.5pF, it is noted that large distortion on the passband at 2.35 GHz which causes the passband became non flat-top passband. Besides, it has a high reflection loss which is more than -10dB in the passband.

Hence author chose 0.5pF as the final value capacitor, C_2 for the proposed configuration. Based on previous chapter, inductors played the main role in the passband performance. Author had divided inductors into two sections where front section inductors indicated L_1 and the behind section of the inductors labelled as L_2.

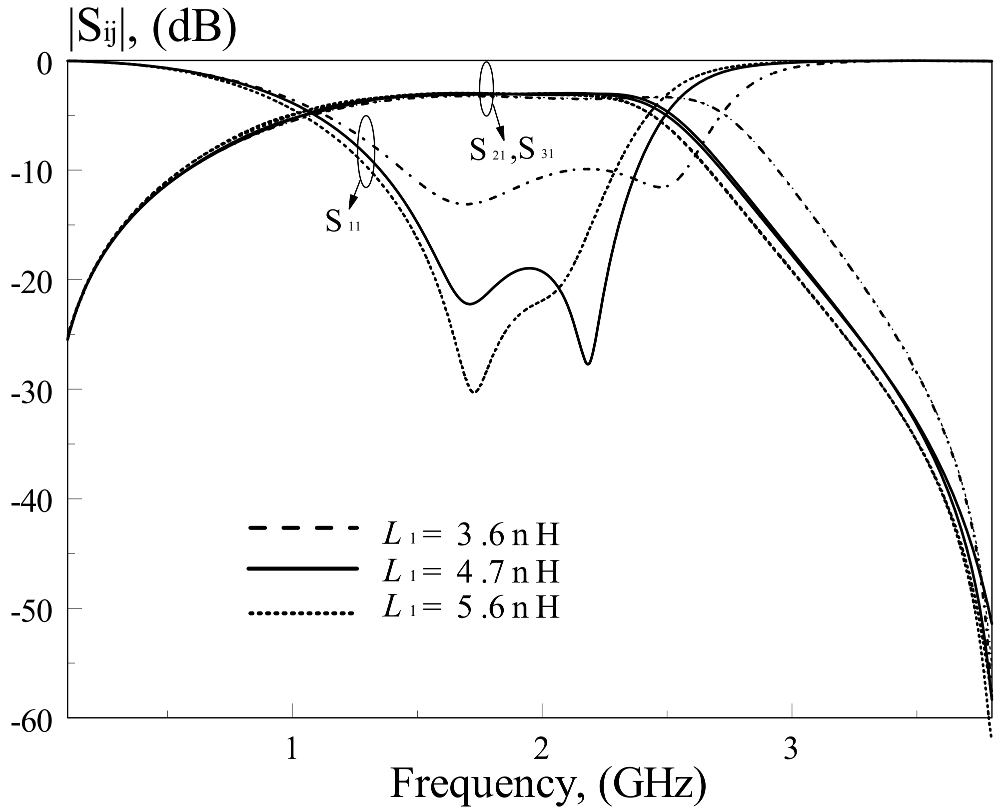

Figure 4.14: Effect of inductance, L_1

Figure 4.14 shows the analysis on inductor, L_1 which value is proposed to be 4.7nH in this design. Three typical values of inductance, 3.6nH, 4.7nH and 5.6nH were simulated. By varying the inductance value to 3.6nH, it can be observed that the return loss, S_{11} is increased more than -10dB due to poor matching.

If the L_1 value is 5.6nH, the return loss, S_{11} will increases to -30dB within the passband problem and it also causes the bandwidth become slightly smaller as the merging of two poles is deteriorated. As a result, 4.7nH is the suitable value for L_1.

Despite inductors, L_1, the analysis also performs on the inductors, L_2 where were located at second section of the prototype. In this case study, author had fixed the inductors values, L_1, and the inductors values, L_2, were manipulated between 2.2nH, 3.6nH and 4.7nH.

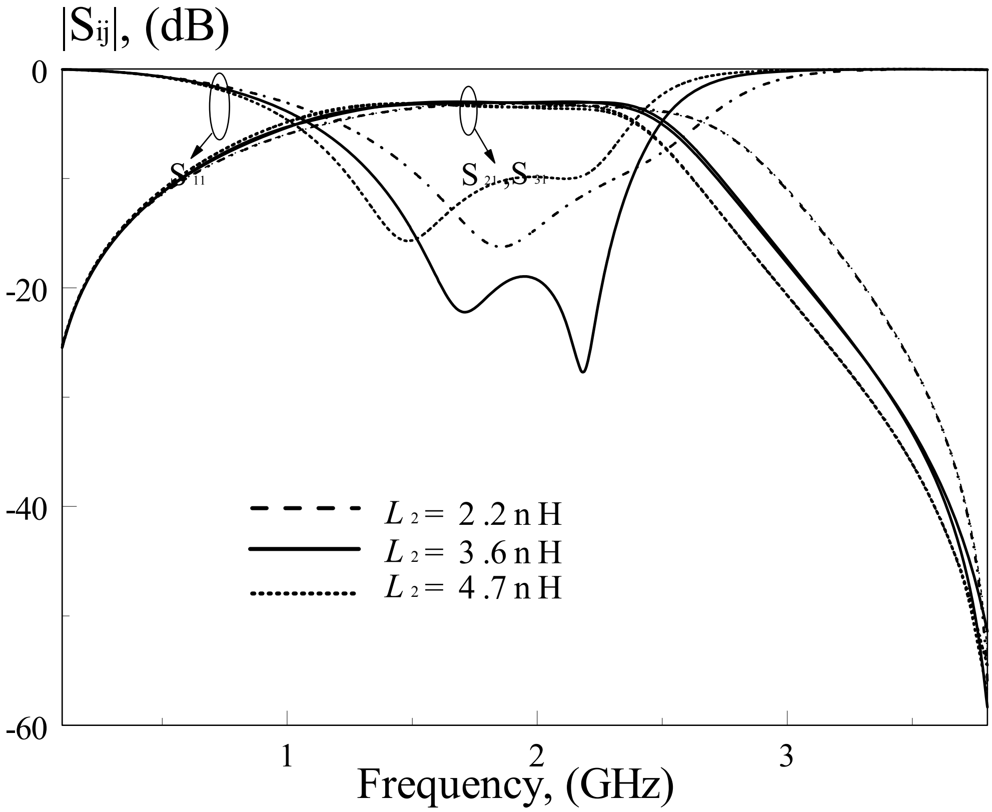

Figure 4.15 Effect of inductance, L_2

. From figure 4.15, it can be observed that, the return loss, S_{11} become lower than -15 dB when L_2 was 2.2nH, while the dual-mode characteristic is deteriorating and caused a narrower passband.

Meanwhile, when L_2 is increased to 4.7nH, the bandwidth of the passband is broadening but the return loss, S_{11} immediately become higher. Again proven that both section of inductors, L_1 and L_2, the values should not be the same.Obviously, the best choice of L_2 value is 3.6nH, which has an acceptable return loss at higher than -20 dB and also larger bandwidth.

CHAPTER 5

CONCLUSION AND RECOMMENDATIONS

5.1 Achievements of the project

In this project, a hybrid lump-element microstrip filter and lump-element microstrip power divider have been proposed and investigated. This proposed design which employed by lump elements has avoided gap issue in fabrication and total layout has reduced by half.

The design technique that employed the lump-element coupling through the configuration is able to produce a high performance bandpass filter and power divider. Therefore, it may be good candidate for many communication applications for which sharp selectivity (lump microstrip square ring) and wideband (lump microstrip coupled line filters, power dividers) are required.

5.2 Recommendations

The configuration of lump microstrip coupled line filter with 1 capacitor is same as 3 capacitors, just the amount lump elements increased. Refer measured results in chapter 3.1 and chapter 3.2, coupled line filter with 1 capacitor has 9.63% larger bandwidth than 3 capacitors. Although just a slightly different, but also indicated that more lumped element will create more unwanted distortion and spend more time on the optimisation. So, one capacitor placing between the gaps of coupled lines is sufficient. Besides, value inductors where replaced the transmission lines should not too high or too low.

Meanwhile, the proposed lump microstrip power dividers is the modified from the lump coupled line filters. The parameters are slightly different. Same as above, lump coupled line power dividers with 1 capacitor has about 10% larger bandwidth than power divider with 3 capacitors. The lump coupled line power dividers perform well in the passband which considered ultra-wide band because fractional bandwidth percentages have achieved more than 100%. This will be very useful in the communication system since more equal outputs of strong signals can be produced.

Lump element idea also applied in reducing layout of square ring as well. The size of square ring has been reduced more than 70% but the frequency selectivity still remains in good performance. Inductor values between the slots of lines are advice to be small as well. Thus, it can further improve by adding one more port to become a power divider, proposed layout has been sketch as below and hope will success in the future.

5.3 Conclusion

The simulated results based on Ansoft HFSS version 8 and AWR software agreed reasonably well with measurements. The objectives of this project have been achieved. Hence, the current project can be further improved by applying lump element to other design for miniature purpose and will be very useful in modern wireless communication systems.

REFERENCES

Ban-Leong Ooi and Ying Wang, “Novel miniaturized open-square-loop resonator with inner split rings loading,” *Microwave Theory and Techniques, IEEE Transactions on* , vol.54, no.7, pp. 3098- 3103, July 2006

Chang, K. (2000). *RF and Microwave Wireless Systems.* John Wiley & Sons, Inc.

E. J. Wilkinson, “An N-Way Hybrid Power Divider”*, IRE Transactions on Microwave Theory and Techniques*, January 1960

Dongke Zh, Yewen Zhang, *Codirectional Coupler and Power Divider Mixed Microstrip and Metamaterials with Lumped-Elements L-C*, Intemational Conference on Microwave and Millimeter Wave Technology Proceedings, 2004.

G.A. Deschamps, “Microstrip Microwave antennas,” *presented at the 3rd USAF sypo-sium On Antennas*, 1953

Hong, J.-S., & M.J. Lancaster. (2001). *Microstrip Filtter for RF/Microwave Applications.* John Wiley & Sons, Inc.

Hunter, I. (2001). *Theory and Design of Microwave Filters.* United Kingdom: The Institution of Electrical Engineers.

J.Q.Howell, “Microstrip antennas,” *IEEE Trans.AP-S Int.Symp.Digest*, pp. 177-180,1972

J.R. James, P.S. Hall, and C.Woods, “Microstrip antenna theory and design,” *Peter peregrinus*, 1981

Jia-Sheng Hong, M.J. Lancaster. (2001). *Microstrip Fitlers for RF/Microwave Applications.* John Wiley & Sons, Inc.

Kin-Lu Wong, *Compact and Broadband Microstrip Antennas*,USA:Wiley,2002.

M.D. Abouzahara and K.C. Gupta, "Multipart power divider/combiner circuits using circular microstrip disk configurations," *IEEE Trans Microwave Theory Tech MTT-35*, 1987

Misra, Devendra, *Radio Frequency and Microwave Communication Circuits: Analysis and Design, 2nd Edition*,USA:Wiley,2004

Mitu, S.S.I. and Taiwo, S.L. (2010, July 11). Multilayer Unequal Microstrip Power Divider. *Antennas and Propagation Society international Symposium (APSURSI)*, 2010 IEEE , 1-4

P.K. Singh, S. Basu and Y.-H. Wang, "Coupled line power divider with compact size and bandpass response," *Electronics Letters* , vol.45, no.17, pp.892-894, Aug. 13 2009 doi: 10.1049/el.2009.1488

Pozar, D. M. (1998). *Microwave Engineering.* John Wiley & Sons, Inc.

Qing-Xin Chu, Li Fan and Huan Wang, "A compact bandpass filter using lumped coupling elements between input port and output port," *Microwave Conference, 2009. EuMC 2009. European* , vol., no., pp.571-574, Sept. 29 2009-Oct. 1 2009

Roberto Frias, "1.7GHz Coupled-line Bandpass Filter," from http://paginas.fe.up.pt/~hmiranda /etele/microstrip/cpl_line_bpf_1.pdf

Ting-Shan Lv, Si-Weng Fok, Cheong P., Kam-Weng Tam, "Compact microstrip square-loop dual-mode bandpass filter design with wideband response," *Circuits and Systems, 2008. APCCAS 2008. IEEE Asia Pacific Conference on* , vol., no., pp.93-96, Nov. 30 2008-Dec. 3 2008

APPENDICES

APPENDIX A: Photos of the proposed lump microstrip coupled line filters.

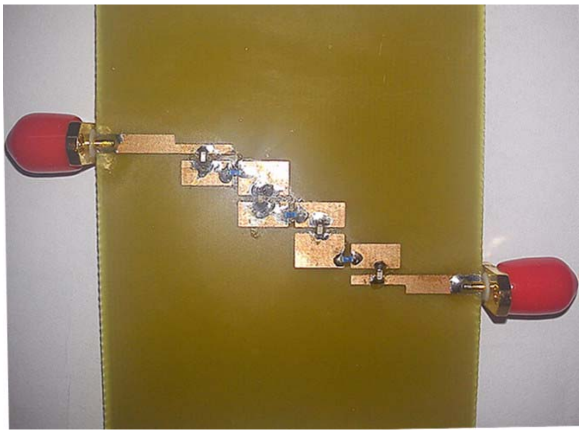

Lump microstrip coupled line with 1 capacitor filter

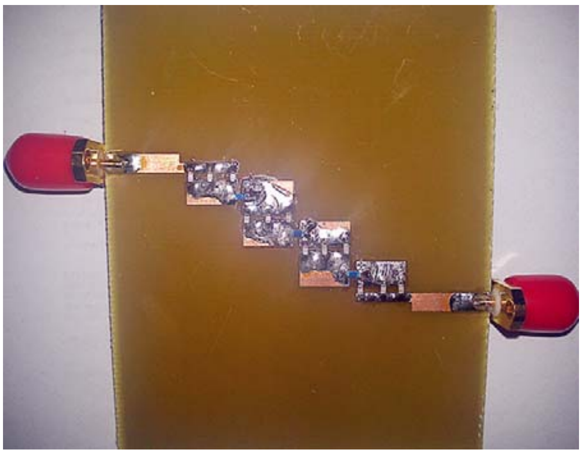

Lump microstrip coupled line with 3 capacitors filter

APPENDIX B: Photos of the proposed lump microstrip square ring filters.

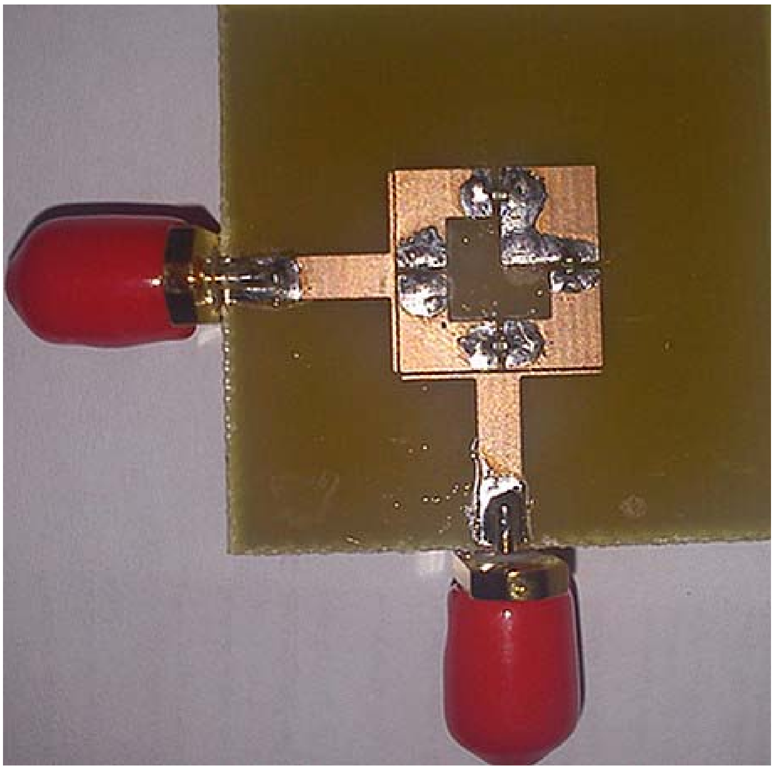

Lump microstrip square ring filter

APPENDIX C: Photos of the proposed lump microstrip coupled line power dividers

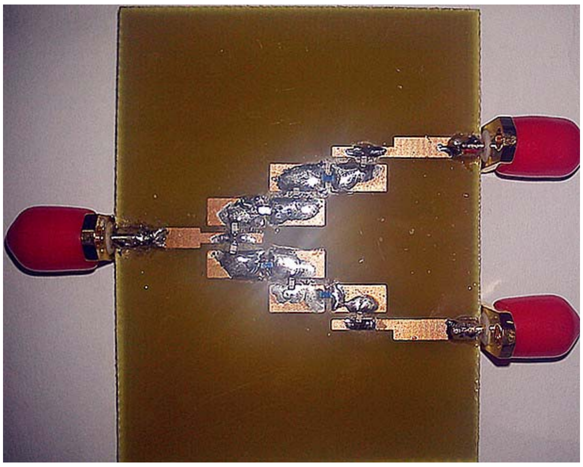

Lump microstrip coupled line with 1 capacitor power divider

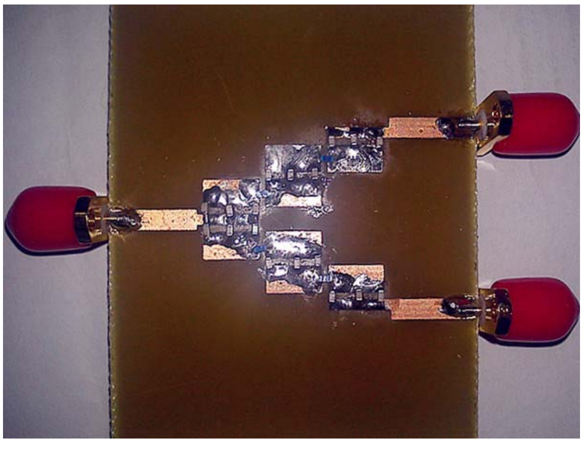

Lump microstrip coupled line with 3 capacitors power divider